A SEMI-CLASSICAL METHOD FOR HEAVY ION COLLISIONS

Thesis Submitted for the Degree
of
Doctor of Philosophy (Science)
of
The University of North Bengal
1985

BY
RANJIT KUMAR SAMANTA

ST - VERP

STOCK TAKING - 2011

T O

MY GRAND MOTHER

A N D

MY PARENTS

PREFACE

The thesis contains the results of the work done during the last five years in the Department of Physics, North Bengal University. A part of the results has already been published. I wish to record my gratitude to Dr. S. Mukherjee, Professor of Physics for his constant guidance and inspiration. I am thankful to the authorities of the Department of Physics,N.B.U., for extending me the necessary facilities. I am also thankful to Professor P.C.Sood and Dr. C. Maheswari of Banaras Hindu University for various help and collaboration for a part of the work and to Professor D.A. Bromley, Wright Nuclear Structure Laboratory, Yale University, for sending me the experimental data on $^{16}O - ^{16}O$ scattering. I am indebted to Dr. D. P. Datta, Mr. A. K. Roy and Mr. A. K. Guha and other members of the Department of Physics for numerous help and to Mr. S.Choudhury for typing the thesis. I would also like to acknowledge the University of North Bengal for awarding me a University Fellowship. Moreover, I would like to record my gratitude to Professor B. Majee, Convener, Department of Computer Science and Application and to Professor N. Chaudhuri, Department of Physics for their encouragement. I shall record my heartiest gratitude to my uncle, Sri Sasanka Sekhar Samanta for his guidance since my school days. Lastly, I must thank my wife, Joyashri, who always encouraged me to spend odd hours with my research work.

Ranjit Kumar Samanta
(Ranjit Kumar Samanta)

Raja Rammohunpur,

February 22 ,1985.

TABLE OF CONTENTS

PAGE

CHAPTER I

INTRODUCTION

I.1. Introduction

Heavy ion collision experiments present a rapidly developing field of research in atomic and nuclear physics. It is now possible to study atomic physics far beyond the region of stable elements. This includes the interesting electrodynamic phenomena associated with an overcritical coulomb field[1-5] that can effectively be obtained when two heavy ions (atoms) come close enough to form, for a short while, a quasi molecule. It has been recognised that a careful study of the positrons emitted from this system should be able to provide useful information regarding the basic problem of the interaction of an electron with a strong coulomb field. Although conventional perturbation techniques are not applicable here, significant progress has nevertheless been achieved in interpreting qualitatively the accumulating data on the over critical field problem. The interpretation of the results is, however, complicated because of the fact that positrons may be produced through a number of mechanisms. Apart from a spontaneous decay of the neutral vacuum[6] there is the possibility of dynamically induced transitions between adiabatic electronic states, leading to positron emission. This may occur also for states that are not overcritical. Positrons produced by these processes, are, however, distinguishable. While the positrons produced in spontaneous vacuum decay should have the energy of the

bound state resonance, the energy spectrum in the induced decay should be much broader. Positrons could also be produced as a 'shake-off' of the strong vacuum polarization cloud[7] close to the nuclei. Lastly, positrons could be produced as a result of nuclear processes. Thus, one of the nuclei could be coulomb excited and the high energy photon emitted could be internally converted. It is obvious that a careful study of all these processes should be made before one can confirm the theoretical concepts. The strong time-dependence of the collision process plays an important role in the theoretical formulation of the problem. During the collision, the length of the vector $\vec{R}$ connecting the two nuclei changes in time and $\vec{R}$ also undergoes a rotation. Some relief, however, comes through the fact that the motion of the nuclei can be described to a good accuracy from a semiclassical consideration, and in some cases, simply by Rutherford scattering formula.

Apart from atomic physics, heavy ion experiments have also opened up new fields of study in nuclear physics. The nucleus has now been subjected to much more severe perturbations than were earlier possible with lighter projectiles. New reaction processes have become accessible owing to the availability of higher kinetic energy and angular momentum. Also, the search for exotic phenomena like the production of shock waves and superdense matter with the associated phase transition

is continuing. Although the studies of proton and pion spectra and their multiplicities have not yet given any signal for the occurance of these phenomena, the possibilities are not yet ruled out. Some progress has also been made in the study of very neutron rich light nuclei using heavy ion reactions at low energies[8]. The study of nuclear states with high angular momenta has become another subject of interest in heavy ion physics. Also, the possibility of transferring a large number of particles provides a new technique to probe into excited states of nuclei. These deep inelastic transfer phenomena have also been studied within the frame work of statistical mechanics with remarkable success. It is expected that the studies on the entire range of heavy ion reactions, elastic, inelastic, transfer phenomena and fusion will provide us a deep insight into the properties of nuclei and the nature of nuclear force in near future. The heavy ion reactions herald the begining of a new area of physics, which will develop, giving rise to many new concepts as the experimental information and the theoretical interpretation become more precise.

The collision of two ions or atoms is a complicated many body problem and a detailed analysis is called for to extract the relevant information from the heavy ion data. A crucial role is played by the elastic scattering cross-section. Attempts have been

made to study various elastic scattering processes assuming different optical model potentials between the colliding nuclei. It is generally hoped, though not confirmed, that a suitable complex optical potential will suffice to describe the elastic scattering results. The interaction potential may be useful also for solving the equation of motion for heavily damped collision, because the driving force is the gradient of the interaction potential. The concept of scattering from a complex potential has, therefore, been subjected to considerable scrutiny in connection with the heavy ion reactions. The data from elastic scattering experiments with a variety of projectiles and targets are now available and some attempts have been made to fit these data with potential models, mostly of the Woods-Saxon type. Although a direct numerical method of computing the phase shifts and hence the cross-section still remain the most dependable way of studying the heavy ion scattering, it has been realised since the early days of heavy ion physics that semiclassical methods may be quite useful in this field. The large value of the Sommerfeld parameter

$$\eta = \frac{Z_1 Z_2 e^2}{\hbar v}$$

and the large value of the reduced mass induce a more classical behaviour than when the projectile is a light particle. Naturally, considerable attention was paid to the study of heavy ion processes in the semiclassical approach. This also helped

in model building because one could follow the interacting ions during the whole reaction time.

While the extensive work on the semiclassical methods in connection with the heavy ion scattering brought out many new interesting features, no semiclassical method has so far been found suitable for an accurate calculation for a realistic heavy ion scattering. It appears that further work is needed in this field to exploit fully the versatility of the semiclassical approach.

I.2. Aim of the work

The aim of the present work is to study the accuracy and efficacy of a particular semiclassical method, first suggested by Miller and Good, for application to the study of heavy ion elastic scattering. This we intend to do in steps. The accuracy of the method is first checked by considering some simple real as well as complex potentials. The method is next applied to a typical case, viz. ^{16}O - ^{16}O elastic scattering. The emphasis has been on testing the applicability and thus highlighting the practical difficulties, if any, in working with the semiclassical method, rather than studying the ^{16}O - ^{16}O scattering process very accurately. Thus, we have considered the optical model potential obtained by

Maher et al[9], although it is known that this potential does not fit the experimental data for energies greater than 25 Mev. We have considered a simple generalization of the Miller-Good method suitable for complex trajectories and the extensive work of Knoll and Schaeffer in this field has been very useful in choosing the contributing trajectories when more than one turning points are relevant.

I.3. Summary of the work

The scheme of presentation is as follows:

(a) In Chapter II, we have discussed briefly the Miller-Good semiclassical method and its generalization for complex trajectories, which we intend to apply for the study of some scattering phenomena, including a typical heavy ion elastic scattering process.

(b) In Chapter III, we have applied the Miller-Good method to two types of potentials: (i) real potentials like Ywkawa and Exponential and its complex generalization and (ii) a complex potential of the type $\frac{a}{r} - \frac{i\beta}{r^2}$. The calculated results for the real potentials were compared with exact results and the accuracy of the method for real potentials were checked. The complex potential (ii) is interesting also because the relevant Schrödinger equation is exactly solvable and the exact complex phase shifts can be obtained analytically. The generalized

semiclassical method is then applied to this potential. The semiclassical phase shifts have been shown to be fairly accurate over a wide range of values of the parameters, and even at fairly low energies. This encourages one to apply the method to the study of realistic problems, e.g. heavy ion scattering phenomena.

(c) In Chapter IV, we have first considered the effect of the nuclear coulomb field in the ^{16}O - ^{16}O elastic scattering by applying the real Miller-Good method, and treating the absorptive part of the potential perturbatively. In calculating heavy ion scattering cross-section, it has been the usual practice to treat the coulomb effect approximately. Thus the potential taken is obtained either by (a) considering a point charge and a sphere of uniform charge density or (b) that between two uniformly charged spheres. When the nuclei are heavy and have Fermi type of charge distributions, the approximation is a good one. But it is not obvious that the approximation will be valid for light nuclei like (^{12}C, ^{16}O etc.) in the region where the charges overlap. We have, therefore, made semiclassical calculations taking two types of charge distributions: (i) uniform and (ii) modified harmonic well distribution, which is the accepted distribution for p-shell nuclei. It has been seen that the difference of phase shifts in the two cases is noticeable at least for some low L values.

The cross-sections in general do not show much difference. However, it has been pointed out that there is some justification for choosing the realistic charge distribution for light nuclei like ^{12}C, ^{16}O when one tries to fit an entire range of experimental results of heavy ion scattering, like elastic scattering, transfer phenomena, fusion etc.

We have next applied the complex Miller-Good method to study a typical ^{16}O - ^{16}O elastic scattering phenomena at a high energy. The prescription of Knoll and Schaeffer has been followed in the selection of important trajectories. The perturbative method of treating complex potential has also been considered for this problem. The two results have been compared. The difficulties in applying a complex semiclassical method for a quantitative calculation have been pointed out. Our conclusions are also summarized.

I.4. Computational work

We have written down two programs for calculating (i) the phase shifts by the semiclassical Miller-Good method including the first order correction term in $\hbar^2$ for some simple potentials and (ii) a program to calculate the phase shifts and cross-sections for elastic scattering of p-shell nuclei with complex trajectories for cases where there is contribution from only one complex turning point. The charge distribution could

be either (i) uniform or (ii) modified harmonic well type. The phase shifts have been calculated explicitly upto L = 100 and for higher L, the phase shifts have been assumed to be given by those of the coulomb field. The cross-section has been symmetrized for identical nuclei and the ratio of the cross-section to Mott scattering cross-section has also been computed.

REFERENCES

1. W. Pieper, W. Greiner, Z. Phys. 218, 327 (1969).
   B. Müller, H. Peitz, J. Rafelski, W. Greiner, Phys. Rev. Lett. 28, 1235 (1972).
   B. Müller, J. Rafelski, W. Greiner, Z. Phys. 257, 62 u. 183 (1972).
2. H. Peitz, B. Müller, J. Rafelski, W. Greiner, Lett. Nuovo Cim. 8, 37 (1973).
3. K. Smith, H. Peitz, B.Müller, W. Greiner, Phys. Rev. Lett. 32, 554 (1974).
4. J. Rafelski, L.P. Fulcher, W. Greiner, Phys. Rev. Lett. 27, 958 (1971).
   J. Rafelski, B. Müller, Phys. Rev. Lett. 36, 517 (1976).
5. S.S.Gershtein, Ya.B. Zeldovich, Sov. Phys. JETP 30, 358 (1970).
   Ya. B. Zeldovich, V.S. Popov, Sov. Phys. Usp. 14, 673 (1972).
   V.S. Popov, Sov. J. Nucl. Phys. 15, 595 (1972).
6. Berndt Müller, R.K.Smith, and Walter Greiner, Atomic Phys. 4, pp. 209, Ed. G.Zu Putlitz, E.W. Weber and A. Winnacker (Plenum Publishing Corporation).
7. Gerhard Soff, Joachim Reinhardt, Berndt Müller, and Walter Greiner, Phys.Rev.Lett. 38, 592 (1977).
8. A.G.Artukh, Nucl. Phys. A176, 284 (1971).
9. Maher et al, Phys. Rev. 188, 1665 (1969).

CHAPTER II

COMPLEX MILLER - GOOD METHOD

II.1. Introduction

The JWKB semiclassical approximation is one of the most versatile techniques of quantum mechanics. The applicability of the method, however, could not be fully exploited because of a serious drawback which shows up at the classical turning points, i.e. points where the classical velocity of the particle vanishes. Unfortunately, classical turning points appear in most problems of physical interest. In a scattering event, the incident wave is reflected from at least one turning point, whereas for a bound state, there are at least two turning points. The JWKB wave function becomes singular at these points. In order to get a finite wave function, one has to make use of the connection formula across the turning point. Also, the correction terms of higher order in $\hbar^2$ diverge badly at the turning points. The method is suitable for potentials which vary so slowly that the momentum of the particle remains nearly constant over many wavelengths. The method obviously fails when the particle energy is low.

To overcome these difficulties, Miller and Good[1] proposed a modification of the JWKB method. The method has been developed further by a number of workers, Rosen and Yennie[2], Lu and Measure[3], Wald and Lu[4] and Berry and Mount[5]. The first step in this method is to choose a 'model equation' which is exactly solvable and also similar to the equation to be solved. The solutions of both the equations should have similar behaviour

asymptotically. It is the difference in their asymptotic phases which will be determined by a semiclassical approximation. It is no longer necessary to use any connection formula across the turning points.

The generalized Miller - Good method even with only the first order correction term is fairly accurate. This has been tested for real potentials by a number of authors[6,7,8]. In the next chapter we shall also consider a few simple cases to exhibit the accuracy and the efficacy of the method. The application of the method to a complex potential, however, needs further consideration. The role of complex trajectories in the semiclassical approach has been a subject of intensive study by Balian and Bloch[9], Knoll and Schaeffer[10], Koeling and Malfliet[11], Rowley and Marty[12], Brink and Tagikawa[13] and a number of other authors[14]. Their results are not, in general, directly applicable to the complex Miller-Good (CMG) method. In the latter case, only the difference in phases are determined by the semiclassical method, while in the former, the phase shift is determined directly. However, the role of complex trajectories in the Miller-Good method remains to be studied.

The presentation will be as follows. The method has been briefly reviewed in section II.2. In section II.3, we shall consider a generalization of the method for a complex potential, with special reference to a Woods-Saxon potential.

II.2. Miller-Good method for a Real potential

Let us assume that it is possible to write the Schrödinger radial equation for the problem as

$$\left(\frac{d^2}{dy^2} + \frac{t_1(y)}{\hbar^2} \right) G(y) = 0. \quad \ldots(2.1)$$

Consider another equation

$$\left(\frac{d^2}{ds^2} + \frac{t_2(s)}{\hbar^2} \right) u(s) = 0, \quad \ldots(2.2)$$

which permits an exact solution. We shall call equation (2.2) a 'model equation' for the problem, provided $t_1(y)$ and $t_2(s)$ are 'similar' in the following sense:

(1) They should have equal number of turning points, i.e. for every real physical y_t, which makes $t_1(y_t) = 0$, there should be a real, physical s_t giving $t_2(s_t) = 0$. It is also desirable that the two functions should have the same number of extrema, a condition which is useful when higher order corrections are taken into account.

(2) The two functions should have similar behaviour near the respective singular points. However, fairly accurate phase shifts can be obtained in some cases, even when this condition is not satisfied, particularly in cases where the singularity is in the classically inaccessible region. We shall return to this point later on.

If both these conditions are satisfied one considers a transformation T (y) so that

$$G(y) = T(y)\, u\,[\, s(y)] \qquad \ldots(2.3)$$

where s is considered to be a function of y. Substituting (2.3) into equation (2.1) and making use of the equation (2.2), we get the consistency condition

$$s'^2 t_2 - t_1 = \hbar^2 \frac{T''}{T} , \qquad \ldots (2.4)$$

and

$$\frac{T'}{T} = -\frac{1}{2} \frac{s''}{s'} , \qquad \ldots(2.5)$$

where the primes imply differentiation w.r.t. the respective arguments. A solution of (2.5) is found easily

$$T = \frac{1}{\sqrt{s'(y)}} . \qquad \ldots(2.6)$$

Substitution of (2.6) into the equation (2.4) gives

$$s'^2 t_2 - t_1 = \frac{\hbar^2}{4}\left[3 \frac{s''^2}{s'^2} - 2 \frac{s'''}{s'}\right] . \qquad \ldots (2.7)$$

We may now expand s (y) and $t_2(s)$ in powers of $\hbar^2$ and consider terms upto a given order in $\hbar^2$ to satisfy the condition (2.7). Thus the condition can be written

as follows:

(i) to the lowest order in $\hbar^2$:

$$\sqrt{t_1(y)}\, dy = \sqrt{t_2(s)}\, ds \qquad \ldots (2.8)$$

which may be integrated to obtain

$$\int_{y_t}^{y} \sqrt{t_1(y)}\, dy = \int_{s_t}^{s} \sqrt{t_2(s)}\, ds \qquad \ldots (2.9)$$

where y_t, s_t are the respective classical turning points.

(ii) The condition (2.7), upto terms of order $\hbar^2$ becomes

$$\int_{y_t}^{y} p_1\, dy + \frac{\hbar^2}{8} \int_{y_t}^{y} \left(3\, \frac{p_1'^2}{p_1^3} - 2\, \frac{p_1''}{p_1^2} \right) dy$$

$$= \int_{s_t}^{s} p_2\, ds + \frac{\hbar^2}{8} \int_{s_t}^{s} \left(3\, \frac{p_2'^2}{p_2^3} - 2\, \frac{p_2''}{p_2^2} \right) ds \,, \qquad \ldots (2.10)$$

with $t_1(y) = p_1^2$, $t_2(s) = p_2^2$. $\qquad \ldots (2.11)$

The integrals in (2.10) appear to be divergent at the lower limit, i.e. at the turning points. Of course, the divergence may be eliminated in some cases by following the method of Bertocchi et al[14], which consists in converting the integrals in (2.10) into contour integrals

in the s (or y) planes. The choice of the contour is as follows. One takes a contour from $\infty - i\epsilon$ to $\infty + i\epsilon$, going round the turning point in a clockwise direction. On integrating by parts and using the result

$$\oint u\,d\omega = \lim_{\epsilon \to 0} \left[u\omega\right]_{\infty - i\epsilon}^{\infty + i\epsilon} - \int_{\infty - i\epsilon}^{\infty + i\epsilon} \omega\, du$$

$$= - \oint \omega\, du \qquad \ldots (2.12)$$

repeatedly, we can eliminate the p_i from the denominator. Going back to the original contour, we obtain, upto terms of order $\hbar^2$,

$$\int_{y_t}^{y} \sqrt{t_1(y)}\, dy + \frac{\hbar^2}{12} \int_{y_t}^{y} \mathcal{Q}\left[t_1\right] \sqrt{t_1(y)}\, dy$$

$$= \int_{S_t}^{S} \sqrt{t_2(s)}\, ds + \frac{\hbar^2}{12} \int_{S_t}^{S} \mathcal{Q}\left[t_2\right] \sqrt{t_2(s)}\, ds\,, \qquad \ldots (2.13)$$

where

$$\mathcal{Q}\left[t_i\right] = \frac{t_i'''' }{t_i'^2} - 4\,\frac{t_i''' \, t_i''}{t_i'^3} + 3\,\frac{t_i''^3}{t_i'^4}\,, \qquad \ldots (2.14)$$

the primes indicating the number of times the functions are differentiated w.r.t. their respective arguments. While the relation (2.14) does not have p_i in the denominator, the problem is solved only if p_i' does not

have any zero within the range of integration. If p_i does have an extremum, one may still try to evaluate the integral, excluding the singularity[4]. It may be emphasized that the singularity appears only because one is considering only upto a given order of $\hbar^2$. If it were possible to consider all terms of all orders, the singularity will cancel out.

(iii) Upto terms of order $\hbar^4$, one may write

$$\int_{y_t}^{y} \sqrt{t_1(y)}\, dy + \frac{\hbar^2}{12}\int_{y_t}^{y} \mathcal{Q}\left[t_1\right]\sqrt{t_1(y)}\, dy - \frac{\hbar^4}{1440}\int_{y_t}^{y} G\left[t_1\right]\sqrt{t_1(y)}\, dy$$

$$= \int_{S_t}^{S} \sqrt{t_2(s)}\, ds + \frac{\hbar^2}{12}\int_{S_t}^{S} \mathcal{Q}\left[t_2\right]\sqrt{t_2(s)}\, ds - \frac{\hbar^4}{1440}\int_{S_t}^{S} G\left[t_2\right]\sqrt{t_2(s)}\, ds \qquad \ldots (2.15)$$

where

$\mathcal{Q}\left[t_i\right]$ is given by equation (2.14) and

$$G\left[t_i\right] = \frac{5\, t_i^{\mathrm{VII}}}{t_i'^{3}} - \frac{44\, t_i^{\mathrm{VI}} t_i^{\mathrm{II}} + 76\, t_i^{\mathrm{V}} t_i''' + 47\, t_i^{\mathrm{IV}\,2}}{t_i'^{4}}$$

$$+ \frac{222\, t_i^{\mathrm{V}} t_i''^{2} + 680\, t_i'''' t_i''' t_i'' + 140\, t_i'''^{3}}{t_i'^{5}}$$

$$- \frac{1540\, t_i'''^{2} t_i''^{2} + 810\, t_i'''' t_i''^{3}}{t_i'^{6}}$$

$$+ \frac{2205\, t_i''' t_i''^{4}}{t_i'^{7}} - \frac{735\, t_i''^{6}}{t_i'^{8}}, \qquad \ldots (2.16)$$

with

$$t_1^{\overline{VII}} = \frac{d^7 t_1}{dy^7} \quad \text{etc.}$$

... (2.17)

It may be useful to indicate how the consistency condition leads to the determination of the phase shift, relevant for the equation (2.1). Suppose the asymptotic behaviour of the functions G(y) and u(s) are written as:

$$G(y) \xrightarrow[y \to \infty]{} \text{Sin}\,(y + f_1(y) + \sigma) \qquad \ldots(2.18)$$

and

$$u(s) \xrightarrow[S \to \infty]{} \text{Sin}\,(s + f_2(s) + \delta). \qquad \ldots(2.19)$$

Since, by assumption the two solutions have similar behaviours at infinity, one may write

$$\sigma = \delta + \lim_{\substack{y \to \infty \\ S \to \infty}} (s - y + f_2(s) - f_1(y))$$

...(2.20)

The right-hand side can be determined from the consistency condition upto a given order of $\hbar^2$. Some applications of this method will be considered in subsequent chapters.

II.3. Generalization for complex potentials

The Miller-Good method outlined in the last section cannot be generalized for complex potentials in a straightforward manner. The difficulty stems mostly from the fact that the turning points are in general complex and also too many in number. With a Woods-Saxon potential, which is commonly used in the optical model treatment of heavy ion collisions, the situation is even worse, there being an infinite number of turning points due to the complex poles of the Woods-Saxon function. One has to decide if all or only some of them will contribute and also to find out how to combine these contributions in calculating the phase shifts.

The first attempt to study the complex potential was rather casual. Instead of writing for the wave vector

$$K(r) = \left[K^2 - \frac{L(L+1)}{r^2} - \frac{2\mu}{\hbar^2} (V_R + i V_I) \right]^{\frac{1}{2}}, \qquad \ldots(2.21)$$

one expands and keeps terms upto first order in V_I. The resulting JWKB expression for the phase shifts involves integration over the real path from the classical turning points, determined entirely by the real potential, the imaginary part contributing only a damping factor to

each of the partial waves. The approximation seems to be reliable for a small absorption. However, as the energy increases, more and more inelastic channels open up, making this treatment completely unsuitable. It was, therefore, necessary to look for an alternative way of studying complex potentials in the semiclassical approach.

Koeling and Malfliet[11] studied this problem and suggested a generalization of the semiclassical method which includes contributions from all possible complex trajectories. Knoll and Schaeffer[10] have studied the problem analytically and showed that it is not necessary to consider all the complex trajectories. Although the results of Knoll and Schaeffer are not directly applicable to the Miller-Good method, it will be useful to recall some of their results. The relative importance of the contributions for single reflections from different turning points and of possible multiple reflections can be estimated following their analysis. Their prescriptions cannot be given in simple mathematical expressions and may even be difficult to use in some cases. In the case of one dimensional problems, one has to study the topology of Stokes lines around the turning points and in cases of higher dimensions one has to consider the topology of saddles, their positions and heights. But in cases of interest to us, i.e. heavy ion scattering, the topological structure will remain almost unchanged in the range of laboratory energies and for any standard model for the optical potential.

It has been shown that in most of the cases only a few of the complex trajectories make dominant contributions.

We consider a specific example to emphasize the point. Let us consider $^{16}O - ^{16}O$ scattering in which the nuclear potential is given by a Woods-Saxon function

$$V_N = \frac{-(V + iW)}{1 + \exp\left(\frac{r - R}{a}\right)}, \qquad \ldots(2.22)$$

with $V = 50$ Mev, and $W = 20$ Mev, $R = 6.05$ fm and $a = 0.6$ fm. If we consider only the real part of the potential including the centrifugal term, the potential has a pocket for some low values of L, but it decreases monotonically for a large L. One, therefore, gets one real turning point r_1 at high energies, but three real turning points $r_1 > r_3 > r_2$ at lower energies. The transition energy between the two cases is given by[15] (for $a \ll R$)

$$E_0 \simeq \tfrac{1}{2} V_c + V \left[(R - 2a)^2 + 2a^2 \right] / 8aR \qquad \ldots(2.23)$$

which for the values chosen is given by $E_0 \simeq 55$ Mev. If we now include the absorptive part, the real turning point r_1 moves into the complex plane, but two other complex turning points r_2, r_3 also appear. While for larger L values, only the complex trajectory from r_1 contributes, at lower L

values, contributions from both r_1 and r_2 will have to be considered. This is the case even at lower energies. This shows clearly that one cannot simply continue the formula for real trajectories into the complex plane to account for the absorptive part of the potential. However, there is some simplification if the absorption is fairly strong. The turning point r_2 is usually well within the potential so that the reflected wave from r_2 is heavily damped. This leaves the contribution from the outer turning point as the dominant one. Knoll and Schaeffer assert that for a fairly good approximation one needs consider only the outer turning point r_1, if the absorptive potential is strong. In chapter IV of this thesis we shall consider heavy ion scattering in which the prescription of Knoll and Schaeffer will be useful.

The observation of Knoll and Schaeffer makes it easy to generalize the Miller-Good method for a realistic heavy ion scattering. We need to locate the outer turning point r_1 and evaluate the integrals occuring in the expressions (2.13) along a complex trajectory. The contour is then distorted without crossing any singularity of $t_1(y)$ as shown in Fig.2.1. The method is applied to various problems in the following chapters. The simplicity of this prescription makes it possible to obtain $\hbar^2$ correction term also by a simple calculation. It should be emphasized that neglect of the contribution from r_2 introduces an error and this may make any higher order calculation meaningless.

Fig. 2.1. The distorted contour for path intigration.

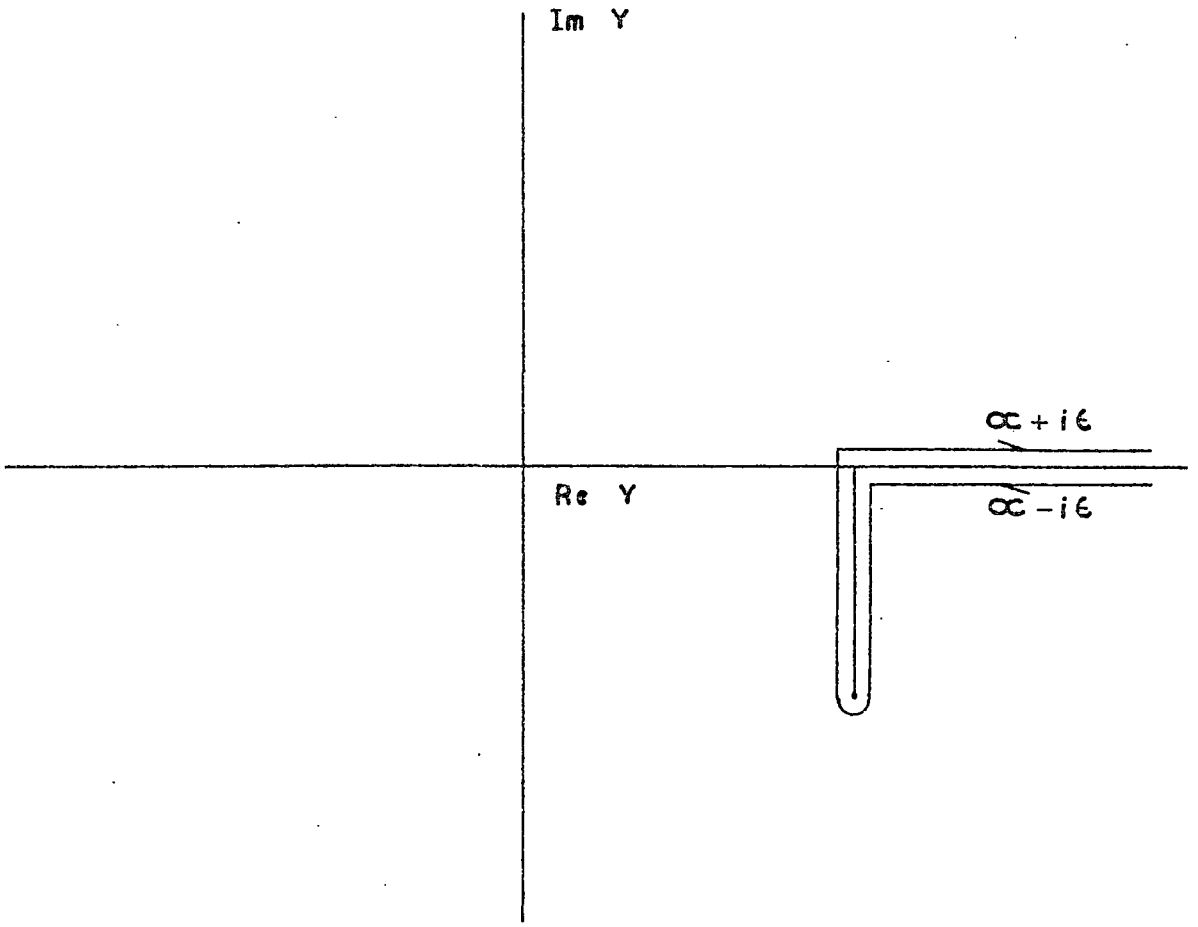

FIG. 2.1 .

REFERENCES

1. S.C. Miller and R.H. Good, Jr., Phys. Rev. 91, 174 (1953).
2. M. Rosen and D.R. Yennie, J. Math. Phys. 5, 1505 (1964).
3. P. Lu and E.M. Measure, Phys. Rev. D5, 2514 (1972).
4. S.S. Wald and P. Lu, Phys. Rev. D9, 2254 (1974).
5. M.V. Berry and K.E. Mount, Rep. Prog. Phys. 35, 315 (1972).
6. S.S.Wald, M. Schardt, and P.Lu, Phys. Rev. D12, 2244(1975).
7. S. Mukherjee and S.S.Chandel, J. Phys. A 11, 1257 (1978).
8. S.S.Chandel and S. Mukherjee, J. Phys. A 12, 329 (1979).
9. R. Balian and C. Bloch, Ann. Phys. (N.Y.) 63, 592 (1971); Ann. Phys. (N.Y.) 85, 514 (1974).
10. J. Knoll and R. Schaeffer, Phys. Lett. 52B, 131 (1974); Ann. Phys. (N.Y.) 97, 307 (1976); Phys. Rep. 31C, 159 (1977).
11. T. Koeling and R.A. Malfliet, Phys. Rep. 22C, 181 (1975).

12. N. Rowley and C. Marty, Nucl. Phys. A 266, 494 (1976).

13. D.M. Brink and N. Tagikawa, Nucl. Phys. A 279, 159 (1977).

14. L. Bertocchi, S. Fubini and G. Furlan, Nuovo Cimento 35, 599 (1965).

15. R. Schaeffer, Les Houches, Session XXX, 1977. Ions lourds et mésons en physique nucléaire/Nuclear Physics with heavy ions and mesons. Edited by R.Balian et al. North-Holland Publishing Co.,1978.

CHAPTER III

SIMPLE POTENTIAL SCATTERING

III.1. Introduction

The semiclassical method discussed in the previous chapter has already been applied to some problems involving real potentials[1,2]. The method has remarkable simplicity and a fair degree of accuracy and, therefore, appears to be a suitable candidate for adaptation for a complex potential. To study the efficacy of the method for a complex potential, we have considered in this chapter three simple examples:

(A) The first example[3] involves a potential consisting of a repulsive coulomb term and an imaginary term of the form $i\beta/r^2$. The Schrödinger radial equation with this potential can be solved exactly and the phase shifts can be obtained analytically. The semiclassical phase shifts, obtained by complex Miller-Good method, (CMG) have been shown to agree very well with the exact phase shifts. We have also studied the variations of the phase shifts with β, which gives the strength of the absorptive part. Although the heavy ion potential is much more complicated than this potential, both share the common feature of a short range absorptive part and a long range coulomb tail. To check the accuracy of the CMG method we have also considered two other[4] simple examples:

(B) Exponential: $V = - V_0 e^{-\gamma r}$ and (C) Yukawa: $V = - \frac{V_0}{r} e^{- \gamma r}$.

The semiclassical phase shifts calculated for real potentials of type (B) and (C) have been compared with their exact values (obtained numerically) and also with some other results obtained by different approximation methods. The semiclassical method gives fairly accurate phase shifts, even at lower energies, say for $K \backsim 1$ fm^{-1}. The potentials were then made complex by making V_o complex, and the CMG phase shifts were computed. For the sake of completeness, we have also presented a treatment of the complex potential, in which the imaginary part of the potential is treated as a perturbation and only terms of the first order are considered. The method, as expected, is accurate only for a small absorption.

III.2. An exactly solvable model

We shall consider here the scattering from a potential $\alpha/r - i\beta/r^2$. The presentation of the results will be as follows. In the sec. III.2.1, the problem has been studied exactly. The section III.2.2 gives the semiclassical treatment for the same problem, while the section III.2.3 gives the perturbative treatment. In section III.2.4, the semiclassical as well as perturbative results have been presented and compared with the exact results.

III.2.1. Exact complex phase shifts

The radial Schrödinger equation with a potential $V(r) = \alpha/r - i\beta/r^2$ is given by

$$\frac{1}{r^2}\frac{d}{dr}\left[r^2\frac{dR_L}{dr}\right] + \left[K^2 - \frac{2nK}{r} - \frac{L(L+1) - i\beta}{r^2}\right] \times R_L(r) = 0, \qquad \ldots(3.1)$$

where

$$n = \frac{\mu ZZ' e^2}{\hbar^2 K}, \quad K = (2\mu E/\hbar^2)^{1/2}.$$

Let $\ell = p + iq$, $p > 0$, be a solution of the equation

$$\ell(\ell + 1) = L(L + 1) - i\beta. \qquad \ldots(3.2)$$

Let us make the substitution

$$R_L(r) = r^{\ell} e^{iKr} f_{\ell}(r)$$

in Eq. (3.1), which gives

$$r f_{\ell}''(r) + (2iKr + 2\ell + 2) f_{\ell}'(r) + \left[2iK(\ell + 1) - 2nK\right] \times f_{\ell}(r) = 0. \qquad \ldots(3.3)$$

The solution of this equation can be written as

$$f_{\ell}(r) = C_{\ell}\, {}_1F_1(\ell + 1 + in, 2\ell + 2, -2iKr), \qquad \ldots(3.4)$$

where C_ℓ is the normalization constant. We will have to impose the appropriate boundary condition on (3.4). In particular, one has to ensure that there is no attenuation of the incoming wave. The asymptotic form of $R_\ell(r)$ is then given by

$$R_\ell(r) \rightarrow C_\ell \frac{\Gamma(2\ell+2)}{(2K)^\ell \, Kr} \quad \frac{e^{n\pi/2} \; e^{q\pi/2}}{\Gamma(p+1+iq-in)} \quad \frac{1}{2i} \; x$$

$$\left[e^{is} - (A+iB)e^{-is} \right] , \qquad \ldots(3.5)$$

where

$$A + iB = \frac{\Gamma(p+1+iq-in)}{\Gamma(p+1+iq+in)} \; e^{-q\pi} , \qquad \ldots(3.6)$$

and

$$S = Kr - \tfrac{1}{2} p\pi - n \ln 2Kr . \qquad \ldots(3.7)$$

The case of a real coulomb potential is well known. The corresponding solution has the asymptotic behaviour

$$R_L(r) \longrightarrow C_\ell \frac{e^{n\pi/2+i\sigma_L^C} \quad \Gamma(2L+2)}{(2K)^L \, Kr \; \Gamma(L+1+in)} \quad X$$

$$\sin \left(Kr - \frac{L\pi}{2} - n \ln 2Kr + \sigma_L^C \right), \qquad \ldots(3.8)$$

where

$$\sigma_L^C = \arg \Gamma(L+1+in). \qquad \ldots(3.9)$$

Since the imaginary part of the potential vanishes for large r, it should be possible to rewrite the Eq. (3.5) in the form (3.8) with the inclusion of an additional phase shift. We, therefore, define the complex phase shifts $\eta_L = \mu + i\lambda$ through the relation

$$\text{Sin}\left(Kr - \frac{L\pi}{2} - n\ln 2Kr + \mu + i\lambda\right) = \frac{1}{2i}\left[e^{is} - (A+iB)e^{-is}\right]. \qquad \ldots(3.10)$$

The complex phase shifts η_L are then given by

$$\eta_L = (L - p)\frac{\pi}{2} - \frac{1}{2}\tan^{-1}(B/A) + \frac{i}{2}\ln(A^2+B^2)^{\frac{1}{2}}. \qquad \ldots(3.11)$$

The phase shifts η_L have been determined for $n = 0.5$, 2.0 and 10.0 and different values of L and β and have been given in Tables I - III.

III.2.2. <u>The semiclassical method</u>

The Schrödinger radial equation for the problem can be written in the form

$$\frac{d^2\Psi_\ell(y)}{dy^2} + \frac{t_1(y)}{\hbar^2}\Psi_\ell(y) = 0, \qquad \ldots(3.12)$$

where $y = Kr$, $\ldots(3.13)$

and

$$t_1(y) = \hbar^2\left[1 - \frac{2n}{y} - \frac{\ell(\ell+1) - i\beta}{y^2}\right] . \qquad \ldots(3.14)$$

As the model equation, we choose, at the first instance, the radial equation for scattering from a point charge, with the same Sommerfeld parameter n. The model equation can be written as

$$\frac{d^2\phi_\ell(s)}{ds^2} + \frac{t_2(s)}{\hbar^2}\phi_\ell(s) = 0, \qquad \ldots(3.15)$$

where

$$t_2(s) = \hbar^2\left[1 - \frac{2n}{s} - \frac{\ell(\ell+1)}{s^2}\right] , \qquad \ldots(3.16)$$

The wave functions have the asymptotic forms

$$\Psi_\ell(y) \underset{\substack{\text{Lim} \\ y\to\infty}}{\longrightarrow} \text{Sin}\,(y - \frac{\ell\pi}{2} - n\,\ln 2y + \sigma_{\text{complex}}), \qquad \ldots(3.17)$$

$$\phi_\ell(s) \underset{\substack{\text{Lim} \\ s\to\infty}}{\longrightarrow} \text{Sin}\,(s - \frac{\ell\pi}{2} - n\,\ln 2s + \sigma_c\ ). \qquad \ldots(3.18)$$

Regarding s as a function of y, and using the relation (2.20), we have,

$$\sigma_{\text{Complex}} - \sigma_c = \underset{\substack{y\to\infty \\ s\to\infty}}{\text{Lim}}\,(s - y - n\,\ln\frac{s}{y}) . \qquad \ldots(3.19)$$

We shall use Langer's substitution and the superscript L will indicate that the function t_i have been Langer substituted. There are two complex roots of the equation

$$t_1^L(y) = 0$$

in the present problem. One of these, however, does not qualify as a turning point because it has a negative real part. Let y_t denote the complex turning point for the present problem. The turning point, the trajectory, and the phase shifts are all real for the model equation. It is nevertheless possible to obtain the transformation (2.3). The complex phase shifts in the Zeroth order is given by

$$\sigma^0_{\text{Complex}} = \sigma^C_L + \lim_{\substack{\tilde{y}\to\infty \\ S\to\infty}} \left(s - y - n \ln \frac{s}{y} \right)$$

$$= \sigma^C_L + \int_{y_t}^{\tilde{y}} \left[y^2 - 2ny - (L+\tfrac{1}{2})^2 + i\beta \right]^{\frac{1}{2}} \frac{dy}{y}$$

$$- \left[\tilde{y}^2 - 2n\tilde{y} - (L+\tfrac{1}{2})^2 \right]^{\frac{1}{2}} + n \ln \left\{ \tilde{y} - n + \left[\tilde{y}^2 - 2n\tilde{y} - (L+\tfrac{1}{2})^2 \right]^{\frac{1}{2}} \right\}$$

$$- \tfrac{1}{2} n \ln \left[n^2 + (L+\tfrac{1}{2})^2 \right] - (L+\tfrac{1}{2}) \left[\sin^{-1} \left[\frac{n\tilde{y} + (L+\tfrac{1}{2})^2}{\tilde{y} \left[n^2 + (L+\tfrac{1}{2})^2 \right]^{1/2}} \right] - \frac{\pi}{2} \right]$$

$$+ \frac{i\beta}{2(L+\frac{1}{2})} \left[\sin^{-1} \left[\frac{n\tilde{y} + (L+\frac{1}{2})^2}{\tilde{y} \left[n^2 + (L+\frac{1}{2})^2 \right]^{1/2}} \right] \right.$$

$$\left. - \sin^{-1} \left[\frac{n}{\left[n^2 + (L+\frac{1}{2})^2 \right]^{1/2}} \right] \right] \qquad \ldots(3.20)$$

with σ_L^C given by (3.9). The second term on the right hand side is obtained by a complex integration. The integration contour has been shown in Fig. 2.1 in chapter II. The first order correction term Δ_L is given by

$$\Delta_L = -\frac{1}{12}\int_{S_t}^{\infty} \mathcal{L}\left[T_2(s)\right]\left[t_2^L(s)\right]^{\frac{1}{2}}\,ds + \frac{1}{12}\int_{\eta_t}^{\infty} \mathcal{L}\left[T_1(y)\right]\left[t_1^L(y)\right]^{\frac{1}{2}}\,dy, \qquad \ldots(3.21)$$

where $\mathcal{L}\left[T_i\right]$ is given by (2.14) and

$$T_1 = y^2\, t_1^L(y), \quad T_2 = s^2\, t_2^L(s). \qquad \ldots(3.22)$$

The expression for (3.21) can be simplified to

$$\Delta_L = -\frac{n}{24\left[n^2 + (L+\frac{1}{2})^2\right]} + \frac{n}{8}\int_{\eta_t}^{\infty} \frac{\left[t_1^L(y)\right]^{\frac{1}{2}}}{(y-n)^4}\, y\, dy \qquad \ldots(3.23)$$

and is easily evaluated along the original contour. In Eq. (3.22), $t_1^L(y)$ and $t_2^L(s)$ are given by

$$t_1^L(y) = 1 - \frac{2n}{y} - \frac{(L + \frac{1}{2})^2 - i\beta}{y^2}$$

and

$$t_2^L(s) = 1 - \frac{2n}{s} - \frac{(L + \frac{1}{2})^2}{s^2} . \qquad \ldots(3.24)$$

The semiclassical phase shifts are then obtained as

$$\sigma_L = \sigma^0_{\text{Complex}} + \Delta_L . \qquad \ldots(3.25)$$

It is instructive to repeat the calculations with another model equation, which is given by the radial equation for a field free particle, viz.,

$$\frac{d^2 \phi(s)}{ds^2} + \frac{t_2(s)}{\hbar^2} \phi(s) = 0 \qquad \ldots(3.26)$$

with

$$t_2(s) = 1 - \frac{L(L+1)}{s^2} . \qquad \ldots(3.27)$$

The phase shifts in this case are given by

$$\sigma_L' = \lim_{\substack{y \to \infty \\ S \to \infty}} (s - y + n \ln 2y)$$

$$= \int_{y_t}^{\breve{y}} \left[y^2 - 2ny - (L + \tfrac{1}{2})^2 + i\beta \right]^{\frac{1}{2}} \frac{dy}{y} - n$$

$$- \left[\breve{y}^2 - 2n\breve{y} - (L + \tfrac{1}{2})^2 \right]^{\frac{1}{2}} +$$

$$n \ln \left\{ \breve{y} - n + \left[\breve{y}^2 - 2n\breve{y} - (L + \tfrac{1}{2})^2 \right]^{\frac{1}{2}} \right\} -$$

$$(L + \tfrac{1}{2}) \left[\sin^{-1} \left[\frac{n\breve{y} + (L + \frac{1}{2})^2}{\breve{y} \left[n^2 + (L + \frac{1}{2})^2 \right]^{1/2}} \right] \right.$$

$$\left. - \sin^{-1} \left[\frac{n}{\left[n^2 + (L + \frac{1}{2})^2 \right]^{1/2}} \right] - \frac{\pi}{2} \right]$$

$$+ \frac{i\beta}{2(L + \frac{1}{2})} \left[\sin^{-1} \left[\frac{n\breve{y} + (L + \frac{1}{2})^2}{\breve{y} \left[n^2 + (L + \frac{1}{2})^2 \right]^{\frac{1}{2}}} \right] \right.$$

$$\left. - \sin^{-1} \left[\frac{n}{\left[n^2 + (L + \frac{1}{2})^2 \right]^{\frac{1}{2}}} \right] \right] + \Delta_L' ,$$

...(3.28)

where Δ_L', the first order correction term, is given by

$$\Delta'_L = \frac{n}{8}\int_{y_t}^{\infty} \frac{\left[t_1^L(y)\right]^{\frac{1}{2}}}{(y-n)^4}\, y\, dy \qquad \ldots.(3.29)$$

and $t_1^L(y)$ is given by the Eq. (3.24). The integrations in (3.28) and (3.29) are to be performed along the contour mentioned earlier.

III.2.3. Perturbative treatment

It may be interesting to note at this stage the results that one obtains by the perturbative treatment of the complex potential by the semiclassical method. The real part of the phase shift is obtained by a straightforward application of the JWKB method to the problem under consideration with the real part of the potential only. The real part of the phase shift is given by

$$\mathrm{Re}\,\eta_L = (L+\tfrac{1}{2})\,\frac{\pi}{2} - Kr_o + \int_{r_o}^{\infty}\left[K(r) - K\right] dr,$$

$$K(r) = K\left[1 - \frac{(L+\frac{1}{2})^2}{K^2 r^2} - \frac{V(r)}{E}\right],$$

$$K(r_o) = 0\,, \qquad \ldots (3.30)$$

where r_o is the classical turning point. Obviously, these results cannot be reliable since the real part of the phase shift given by (3.30) is seen to be independent

of β , whereas the exact phase shifts show a fairly good variation as β changes (Tables I - III and Fig. 3.1). The imaginary part of the phase shift in first order in β is given by

$$I_m \eta_L = \frac{\beta}{2} \int_{r_0}^{\infty} \frac{dy}{y^2 \left[1 - \frac{(L+\frac{1}{2})^2}{y^2} - \frac{2n}{y}\right]^{\frac{1}{2}}} \quad \ldots(3.31)$$

The perturbative imaginary phase shifts are compared with exact and semiclassical results for $n = 0.5$ and different values of L and β and are shown in Fig.3.2.

III.2.4. Results and discussions

The CMG phase shifts calculated for $n = 0.5$, 2.0, 10.0 and various β for the two model equations are given in Tables I, II and III. It may be pointed out that both the real and the imaginary parts of the phase shifts agree fairly well with the exact results. The results for $L = 1$ are, however, much better than for $L = 0$. The accuracy improves with higher L. We can draw the following conclusions:

(a) The real part of the phase shift show a significant dependence on the imaginary part of the potential. For $L = 1$ the real part even changes sign as the

Fig. 3.1. The variation of the real and imaginary parts of the phase shifts with β for various values of L.

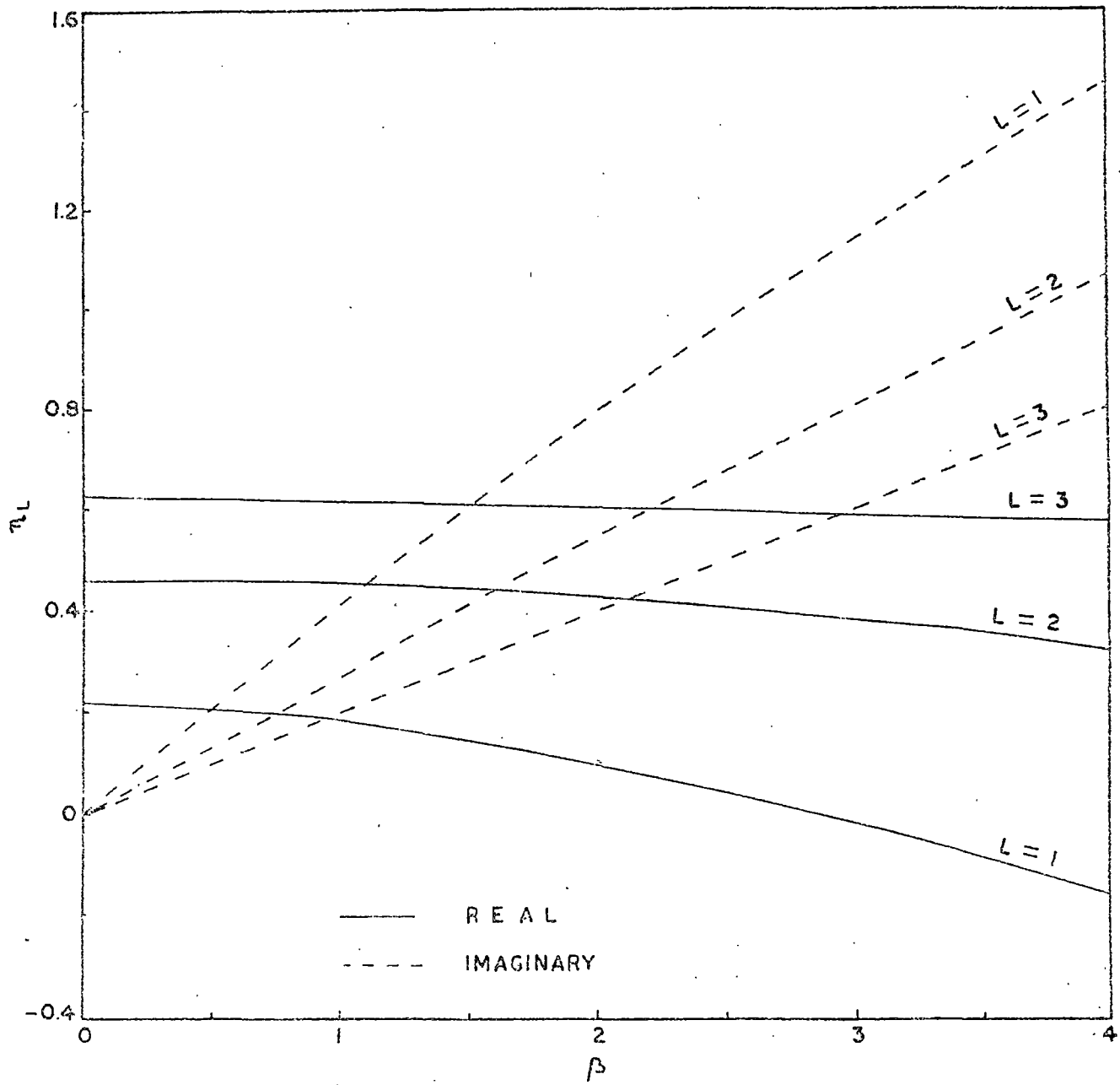

FIG. 3.1.

Fig. 3.2. Imaginary part of the phase shifts obtained by exact numerical, semi-classical and perturbative methods for L = 0 and 1.

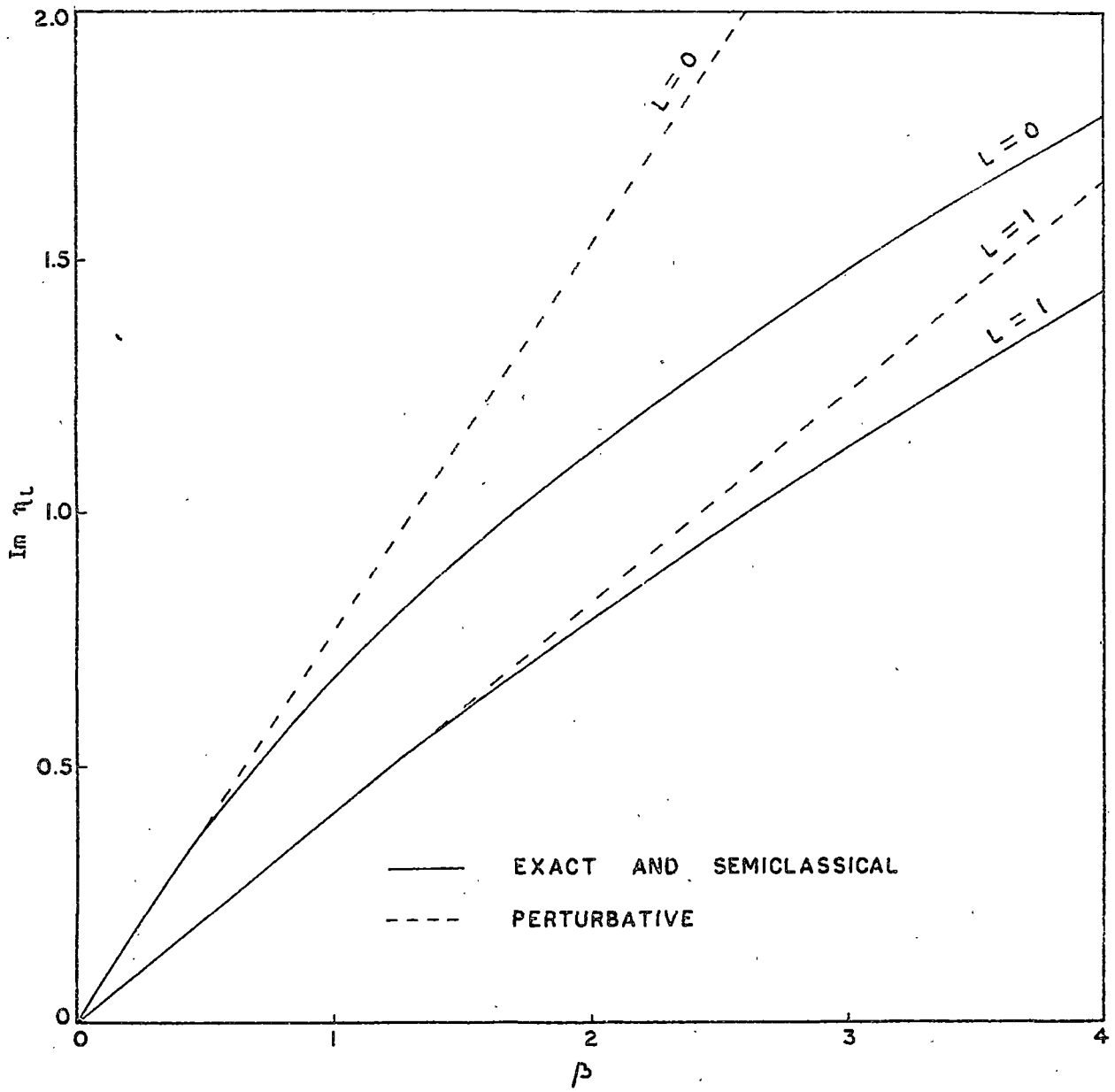
2.0
1.5
1.0
0.5
0
Im η_L
0
1
2
3
4
β
L=0
L=0
L=1
L=1
EXACT AND SEMICLASSICAL
PERTURBATIVE

FIG. 3.2 .

TABLE I. The exact and the semiclassical phase shifts for n = 0.5

β	Real η_L	Real σ_L	Real σ_L'	Imaginary η_L	Imaginary σ_L and σ_L'
			L = 0		
0.00	-0.2441	-0.2441	-0.2389	0.0000	0.0000
0.25	-0.2683	-0.2694	-0.2642	0.2069	0.2071
0.50	-0.3211	-0.3220	-0.3210	0.3873	0.3880
1.00	-0.4492	-0.4498	-0.4496	0.6835	0.6840
1.50	-0.5802	-0.5811	-0.5808	0.9254	0.9263
2.25	-0.7677	-0.7685	-0.7681	1.2287	1.2290
2.50	-0.8273	-0.8280	-0.8277	1.3188	1.3190
3.00	-0.9425	-0.9439	-0.9428	1.4869	1.4870
3.50	-1.0526	-1.0529	-1.0529	1.6419	1.6419
4.00	-1.1582	-1.1589	-1.1584	1.7863	1.7863
			L = 1		
0.00	0.2196	0.2196	0.2200	0.0000	0.0000
0.25	0.2173	0.2172	0.2177	0.1047	0.1048
0.50	0.2106	0.2105	0.2110	0.2089	0.2090
1.00	0.1848	0.1846	0.1851	0.4130	0.4132
1.50	0.1449	0.1446	0.1451	0.6090	0.6093
2.25	0.0660	0.0656	0.0660	0.8843	0.8846
2.50	0.0361	0.0357	0.0361	0.9709	0.9712
3.00	-0.0278	-0.0278	-0.0273	1.1368	1.1370
3.50	-0.0941	-0.0946	-0.0942	1.2934	1.2936
4.00	-0.1630	-0.1635	-0.1631	1.4418	1.4419

Table 1 Contd....

L = 2

β	Real η_L	Real σ_L	Real σ_L'	Imaginary η_L	Imaginary σ_L and σ_L'
0.00	0.4646	0.4646	0.4646	0.0000	0.0000
0.25	0.4640	0.4639	0.4640	0.0688	0.0688
0.50	0.4622	0.4621	0.4622	0.1375	0.1375
1.00	0.4551	0.4550	0.4551	0.2745	0.2745
1.50	0.4435	0.4434	0.4435	0.4105	0.4105
2.25	0.4179	0.4178	0.4179	0.6116	0.6117
2.50	0.4074	0.4073	0.4073	0.6777	0.6778
3.00	0.3835	0.3834	0.3835	0.8083	0.8084
3.50	0.3563	0.3561	0.3562	0.9365	0.9366
4.00	0.3260	0.3258	0.3259	1.0622	1.0622

TABLE II. The exact and semiclassical phase shifts for n = 2.0.

β	Real η_L	Real σ_L	Real σ_L'	Imaginary η_L	Imaginary σ_L and σ_L'
			L = 0		
0.00	0.1296	0.1295	0.1293	0.0000	0.0000
0.25	0.1290	0.1287	0.1285	0.0625	0.0624
0.50	0.1269	0.1267	0.1265	0.1248	0.1247
1.00	0.1188	0.1188	0.1186	0.2487	0.2487
1.50	0.1059	0.1059	0.1058	0.3709	0.3708
2.25	0.0785	0.0785	0.0785	0.5499	0.5498
2.50	0.0675	0.0675	0.0675	0.6082	0.6082
3.00	0.0432	0.0433	0.0432	0.7228	0.7228
3.50	0.0162	0.0162	0.0162	0.8345	0.8345
4.00	-0.0130	-0.0129	-0.0129	0.9433	0.9433
			L = 1		
0.00	1.2368	1.2367	1.2367	0.0000	0.0000
0.25	1.2364	1.2363	1.2362	0.0542	0.0542
0.50	1.2352	1.2351	1.2351	0.1083	0.1083
1.00	1.2304	1.2304	1.2303	0.2162	0.2161
1.50	1.2226	1.2225	1.2224	0.3235	0.3234
2.25	1.2054	1.2054	1.2053	0.4825	0.4824
2.50	1.1983	1.1983	1.1982	0.5350	0.5350
3.00	1.1823	1.1823	1.1821	0.6387	0.6387
3.50	1.1639	1.1638	1.1638	0.7409	0.7409
4.00	1.1435	1.1435	1.1434	0.8415	0.8415

Table II Contd....

L = 2

β	Real η_L	Real σ_L	Real σ_L'	Imaginary η_L	Imaginary σ_L and σ_L'
0.00	2.0222	2.0221	2.0222	0.0000	0.0000
0.25	2.0220	2.0220	2.0219	0.0450	0.0449
0.50	2.0214	2.0213	2.0213	0.0900	0.0899
1.00	2.0189	2.0188	2.0187	0.1799	0.1799
1.50	2.0147	2.0146	2.0146	0.2695	0.2695
2.25	2.0055	2.0054	2.0053	0.4034	0.4034
2.50	2.0016	2.0016	2.0015	0.4478	0.4479
3.00	1.9927	1.9926	1.9926	0.5363	0.5363
3.50	1.9824	1.9824	1.9824	0.6242	0.6242
4.00	1.9706	1.9705	1.9705	0.7114	0.7114

TABLE III. The exact and semiclassical phase shifts for n = 10.0

β	Real η_L	Real σ_L	Real σ_L'	Imaginary η_L	Imaginary σ_L and σ_L'
			L = 0		
0.00	13.8029	13.8030	13.8030	0.0000	0.0000
0.25	13.8029	13.8029	13.8029	0.0125	0.0124
0.50	13.8029	13.8028	13.8028	0.0250	0.0249
1.00	13.8028	13.8028	13.8027	0.0500	0.0500
1.50	13.8027	13.8026	13.8025	0.0750	0.0750
2.25	13.8025	13.8024	13.8023	0.1125	0.1125
2.50	13.8024	13.8024	13.8023	0.1250	0.1250
3.00	13.8022	13.8022	13.8021	0.1500	0.1500
3.50	13.8019	13.8019	13.8018	0.1750	0.1750
4.00	13.8016	13.8016	13.8015	0.1999	0.1999
			L = 1		
0.00	15.2740	15.2741	15.2741	0.0000	0.0000
0.25	15.2740	15.2740	15.2740	0.0124	0.0123
0.50	15.2740	15.2739	15.2739	0.0248	0.0247
1.00	15.2740	15.2739	15.2739	0.0497	0.0496
1.50	15.2749	15.2738	15.2738	0.0745	0.0745
2.25	15.2736	15.2735	15.2735	0.1118	0.1118
2.50	15.2735	15.2735	15.2734	0.1242	0.1242
3.00	15.2733	15.2732	15.2732	0.1490	0.1490
3.50	15.2730	15.2729	15.2729	0.1738	0.1738
4.00	15.2727	15.2727	15.2727	0.1987	0.1987

Table III Contd...

L = 2

β	Real η_L	Real σ_L	Real σ_L'	Imaginary η_L	Imaginary σ_L and σ_L'
0.00	16.6474	16.6475	16.6475	0.0000	0.0000
0.25	16.6474	16.6474	16.6474	0.0123	0.0121
0.50	16.6474	16.6473	16.6473	0.0245	0.0244
1.00	16.6474	16.6474	16.6473	0.0490	0.0489
1.50	16.6473	16.6473	16.6471	0.0735	0.0735
2.25	16.6470	16.6469	16.6469	0.1103	0.1103
2.50	16.6470	16.6469	16.6468	0.1226	0.1226
3.00	16.6467	16.6467	16.6466	0.1471	0.1471
3.50	16.6465	16.6464	16.6464	0.1716	0.1716
4.00	16.6462	16.6462	16.6461	0.1961	0.1961

imaginary potential becomes stronger. The perturbative method, on the other hand, gives a real part which does not depend on the imaginary part, as is evident from Eq. (3.30).

(b) The imaginary part of the phase shift shows a monotonic increase as β increases, though not as fast as is given by the perturbative method. For small values of β, the perturbative results are close to the exact values, but deviate increasingly as β increases. Again, with an increase in L, $I_m \eta_L$ decreases. Physically this means that partial waves with higher L are less absorbed because of the centrifugal barrier.

(c) For the potential considered, the correction term of order $\hbar^2$ is small in the case of the first model equation. But for the second model equation this contribution is significant. This is easy to understand. In the case of the first model equation, there is a cancellation between the correction terms that does not happen in the other case. Terms of higher order in $\hbar^2$ depend on the higher derivatives of the function $t_1(y)$ which are anyway small for the present problem. However, one may consider a potential which changes rapidly in the vicinity of the turning point. The correction terms may be quite large in that case. For higher L, the correction terms become smaller.

(d) As is evident from the tables I - III, both model equations give almost equally good results.

(e) For fixed L and β, the phase shifts increase with the Sommerfeld parameter n. For a large n, the problem is almost the coulomb scattering problem as is evident from Table III.

III.3. Exponential and Yukawa potentials

It may be useful to apply the CMG method to some other simple cases to test the accuracy and the efficacy of the method. This motivated us to consider Exponential and Yukawa potentials:

$$\text{(a) Exponential: } V = - V_o \, e^{- \gamma r}, \qquad \ldots(3.32)$$

and

$$\text{(b) Yukawa : } V = - \frac{V_o}{r} \, e^{- \gamma r} . \qquad \ldots(3.33)$$

First, we have considered the real potentials and compared our results (calculated upto $\hbar^2$ terms) with the exact phase shifts as well as with the results obtained with different approximation methods. The potentials are then made complex by giving V_o a complex value ($V_o = \vartheta + i\omega$). The path integration is done along the contributing complex trajectory. The variations of the real and imaginary parts of the phase shifts with ω have also been studied. The perturbative semiclassical calculation has also been done for the sake of completeness.

III.3.1. Real potentials

The phase shifts for a real potential in the CMG method can be approximated as

$$\delta_L \simeq \int_{y_t}^{\tilde{y}} \sqrt{\Upsilon(y)}\ \frac{dy}{y} - \sqrt{\tilde{y}^2 - (L+\tfrac{1}{2})^2}$$

$$+ (L+\tfrac{1}{2})\ \mathrm{Cos}^{-1}\left(\frac{L+\frac{1}{2}}{\tilde{y}}\right) + \frac{1}{12}\int_{y_t}^{\infty} \mathcal{Q}[\Upsilon(y)]\sqrt{\Upsilon(y)}\ \frac{dy}{y} \qquad \ldots(3.34)$$

where terms of order $\hbar^2$ have been included.

In above, y_t is the turning point and $\tilde{y}$ is a large value of y so that $V\left(\frac{\tilde{y}}{K}\right) \ll 1$. The function $\Upsilon(y)$ is given by

$$\Upsilon(y) = y^2 - \left(\frac{y^2}{K^2}\right) V\left(\frac{y}{K}\right) - (L+\tfrac{1}{2})^2 \qquad \ldots(3.35)$$

and

$$t_1(y) = \Upsilon(y)/y^2 \qquad \ldots(3.36)$$

The $\mathcal{Q}[\Upsilon(y)]$ is given by equation (2.14). In above, Langer's substitution has been made use of. The Schrödinger

equation for a field-free particle has been chosen as the model equation. The calculated phase shifts depend only weakly on the choice of the model equation. The accuracy of this simple formula (3.34) is checked by comparing the calculated phase shifts with the exact phase shifts and also the phase shifts obtained by different approximation methods. We have chosen $K = 1\ fm^{-1}$, and have shown in Table IV the different results. The exact results (A) have been taken from Wojtczak[5]. The other results are: (B) the results obtained by us, (C) the results obtained by Swan[6] using a modified Born's approximation and (D) the approximation results of Wojtczak. It is seen that for both the Exponential and Yukawa potentials, our results are accurate even when the energy is not too high i.e., for $K \backsim 1\ fm^{-1}$. The accuracy improves considerably as L increases.

It may be pointed out that the method is better suited for cases where an exactly solvable model equation is readily available. The model equation should preferably have the same analytic form as the equation being studied. In particular, the two equations should have similar behaviour near their singular points. Even when the natures of singularities are different, the phase shifts calculated by this method often come out fairly accurately, particularly if the singularity is in the inaccessible region (say at the origin). The accuracy of this method prompts one to consider a complex generalization of this method.

TABLE IV. Phase shifts for real potentials with $K = 1.00\ fm^{-1}$.

Potentials	L	A Exact	B Our	C Swan	D Wojtczak
$V = -V_o\ e^{-\gamma r}$	0	1.0890	1.0833	0.9844	1.1588
V_o=5.2283	1	0.3931	0.3907	0.4039	0.3945
γ = 1.5925	2	0.0985	0.0952	0.1103	0.1099
$V = -V_o \frac{1}{r} e^{-\gamma r}$	0	1.1151	1.1517	0.9685	1.2284
V_o= 1.5933	1	0.3983	0.4044	0.4464	0.3822
γ = 0.6279	2	0.1627	0.1658	0.2314	0.1914

III.3.2. Scattering from Complex potentials

The expression (3.34) for phase shifts can be used even when V_o in (3.32) and (3.33) are given complex values. However, some comments are in order. The integral on the R.H.S. is now to be taken on a complex trajectory. The details of path integration are discussed in section II.3. In the general semiclassical theory with a complex potential, there is a problem of choosing the trajectories that will make significant contributions. The problem has been studied by Knoll and Schaeffer[7], particularly in connection with heavy ion scattering. The problem is more acute there because the Woods-Saxon optical potential leads to infinite number of complex turning points. However, Knoll and Schaeffer have given some prescriptions for locating the turning point/points which can make significant contributions. In most cases of physical interest in heavy ion scattering, only one trajectory makes a dominant contribution. At intermediate energies, there is a range of L values when 2 or 3 turning points contribute, but if the absorptive part G_2 is large, the turning points deep inside may not again be important because of a strong absorption. The simple cases we are studying here, of course, present no such problems. The turning point which is to be considered is the analytic continuation of the real root when $G_2 = 0$. The calculated values of some phase shifts for $K = 1.0\ fm^{-1}$ are shown in Tables V & VI.

TABLE V. Complex phase shifts for K = 1.00 fm^{-1}.

Potential: $V = - V_0 e^{-\gamma r}$, $V_0 = \vartheta + i\omega$,

$\vartheta = 5.2283$ and $\gamma = 1.5925$

ω	Re δ_L	Im δ_L
	L = 0	
0.001	1.0394	0.0002
0.01	1.0395	0.0017
0.05	1.0396	0.0088
0.10	1.0399	0.0176
0.20	1.0407	0.0355
0.30	1.0419	0.0535
0.40	1.0435	0.0716
0.50	1.0453	0.0898
	L = 1	
0.001	0.4061	0.0001
0.01	0.4062	0.0011
0.05	0.4064	0.0054
0.10	0.4070	0.0110
0.20	0.4087	0.0223
0.30	0.4110	0.0337
0.40	0.4138	0.0452
0.50	0.4168	0.0567
	L = 2	
0.001	0.0916	0.0000
0.01	0.0916	0.0002
0.05	0.0915	0.0009
0.10	0.0915	0.0018
0.20	0.0914	0.0037
0.30	0.0914	0.0057
0.40	0.0913	0.0076
0.50	0.0912	0.0096

TABLE VI. Complex phase shifts for K = 1.00 fm^{-1}.
Potential: $V = - V_o \frac{1}{r} e^{-\gamma r}$, $V_o = \vartheta + i\omega$,
$\vartheta = 1.5933$ and $\gamma = 0.6279$

ω	Re δ_L	Im δ_L
	L = 0	
0.001	1.1458	0.0007
0.01	1.1459	0.0071
0.05	1.1474	0.0361
0.10	1.1510	0.0733
0.20	1.1626	0.1493
0.30	1.1787	0.2274
0.40	1.1984	0.3074
0.50	1.2209	0.3894
	L = 1	
0.001	0.4057	0.0003
0.01	0.4057	0.0028
0.05	0.4056	0.0144
0.10	0.4055	0.0292
0.20	0.4040	0.0587
0.30	0.4026	0.0881
0.40	0.4006	0.1174
0.50	0.3979	0.1466
	L = 2	
0.001	0.1656	0.0001
0.01	0.1656	0.0010
0.05	0.1655	0.0054
0.10	0.1655	0.0110
0.20	0.1651	0.0223
0.30	0.1648	0.0335
0.40	0.1644	0.0447
0.50	0.1639	0.0559

III.3.3. Perturbative treatment

It has been pointed out in section III.2.3., that when one uses the first order perturbative semi-classical method for complex potential, the real part of the phase shift is independent of ω while the imaginary part is proportional to ω . For complex Exponential potential, the imaginary part of the phase shifts is given by

$$I_m \delta_L = \omega/2 \int_{r_o}^{\infty} \frac{y\, e^{-y/Kd}}{\sqrt{y2 + \vartheta y^2 e^{-y/Kd} - (L + \frac{1}{2})^2}}\, dy \qquad \ldots (3.38)$$

For complex Yukawa potential one gets a similar expression:

$$I_m \delta_L = \omega/2 \int_{r_o}^{\infty} \frac{K\, e^{-y/Kd}}{\sqrt{y^2 + \vartheta y\, K\, e^{-y/Kd} - (L + \frac{1}{2})^2}}\, dy \qquad \ldots (3.39)$$

where r_o is the corresponding turning point. The values of $I_m \delta_L$ obtained from (3.38) and (3.39) have been compared with the CMG values for $K = 1\ fm^{-1}$ and $L = 0$ and are shown in Fig. 3.3.

Fig. 3.3. Imaginary part of the phase shifts for a complex YuKawa potential. The parameters are as in Table VI.

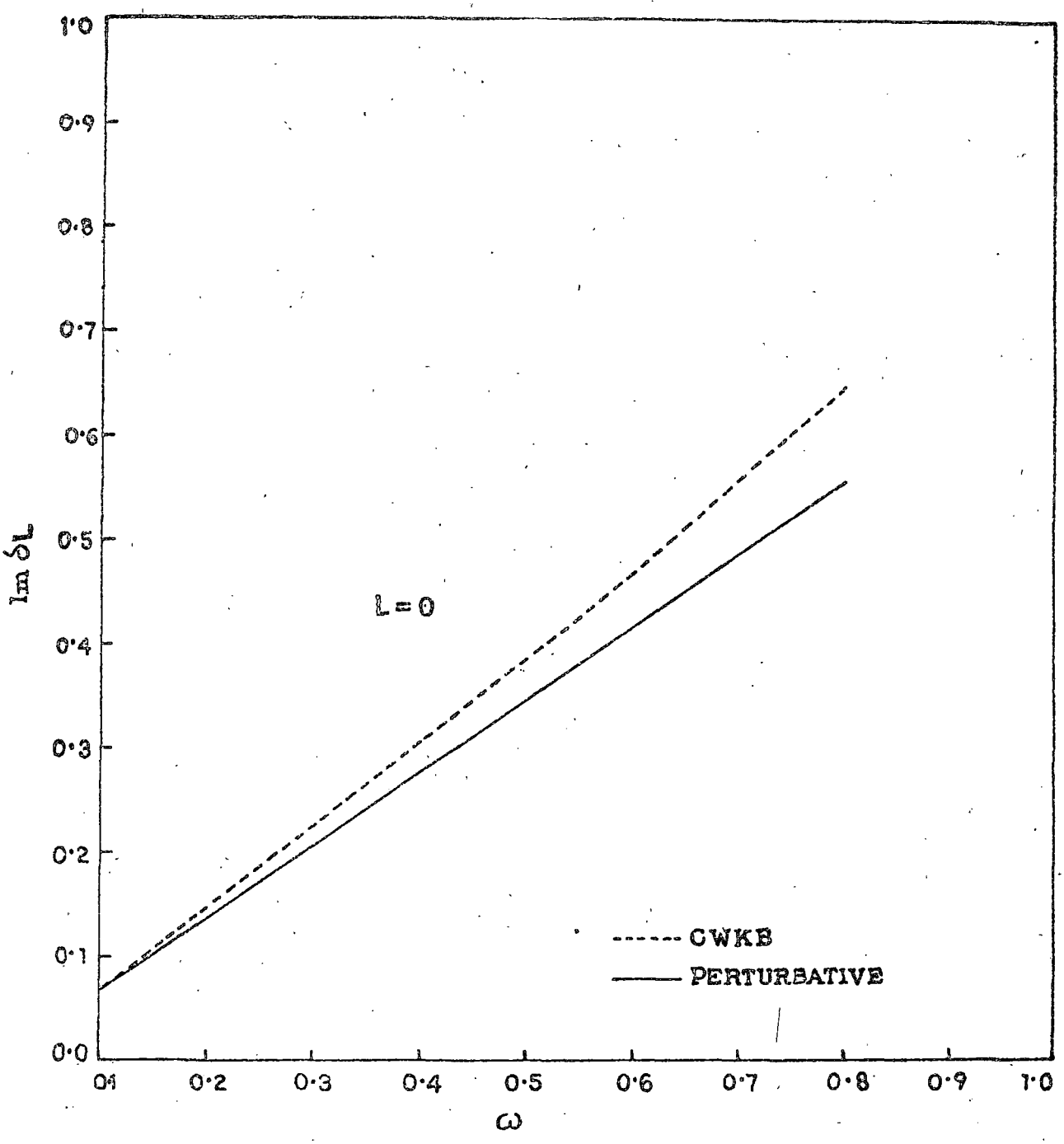
1·0
0·9
0·8
0·7
0·6
0·5
0·4
0·3
0·2
0·1
0·0
Im δL
L=0
------ CWKB
—— PERTURBATIVE
0·1
0·2
0·3
0·4
0·5
0·6
0·7
0·8
0·9
1·0
ω

FIG. 3.3.

III.3.4. Results and conclusions

The study of the Exponential and Yukawa potentials leads to the following conclusions:

1. The semiclassical results calculated by the CMG method are fairly accurate and agree well with the exact results obtained numerically.

2. The real part of the phase shifts varies slowly as ω varies. But the imaginary part shows a rapid change. If one follows a perturbative approach for the imaginary part, one naturally gets, in the first order approximation in ω , a linear relation between $I_m \delta_L$ and ω . This is a good approximation for small ω , as can be seen from Fig. 3.3 also.

3. We have considered here a case where both the real and the imaginary parts of the potential have the same radial dependence. The situation where the radial dependence is different may, in general, be more difficult, as has been pointed out by Schaeffer[8] in connection with a complex Woods-Saxon type potential. The complication is due to the presence of an additional contribution from the sharp edge of the imaginary part of the heavy ion potential.

4. The first order quantum correction is significant here. On the average, the $\hbar^2$ term makes a contribution which is about 3% - 5% of the total phase shifts.

In conclusion, we have shown that the CMG method has the accuracy desirable in a semiclassical calculation for simple potential scattering. For heavy ion scattering, the potentials are, of course, more involved in the sense that more than one turning points may appear. Thus, apart from accuracy, there is also the question of the suitability of the method as a simple working technique. This is the point we would like to study in the next chapter by considering a typical heavy ion scattering experiment.

REFERENCES

1. S. Mukherjee and S.S. Chandel, J. Phys. A. 11, 1257 (1978).
2. S. S. Chandel and S. Mukherjee, J. Phys. A. 12, 329 (1979).
3. R. K. Samanta and S. Mukherjee, Phys. Rev. D26, 2916 (1982).
4. R. K. Samanta, A.K. Roy and S. Mukherjee, Proc. Nucl. and Solid State Phys. Symp. (India), 25B, 164 (1982).
5. L. Wojtczak, Nucl. Phys. 48, 325 (1963).
6. P. Swan, Nucl. Phys. 18, 245 (1960).
7. J. Knoll and R. Schaeffer, Phys. Lett. 52B, 131 (1974); Ann. Phys. (N.Y.) 97, 307 (1976); Phys. Rep. 31C, 159 (1977).
8. R. Schaeffer, Theoretical Methods in Medium energy and heavy ion Physics, eds., K.W. McVoy and W.A. Friedman (Plenum Publishing Corporation), pp. 189 - 234.

CHAPTER IV

APPLICATION: ^{16}O - ^{16}O ELASTIC SCATTERING BY SEMICLASSICAL METHOD

IV. 1. Introduction

Semiclassical methods have already been used extensively in the study of heavy ion collision. The methods have been found quite useful in determining various qualitative aspects of the collision phenomena. However, the accuracy of the semiclassical results in most of the cases are not satisfactory. We intend to study here the applicability as well as the accuracy of the generalized Miller-Good method by considering a realistic problem e.g. $^{16}O - ^{16}O$ elastic scattering. We have considered this problem in two parts. First, we have applied the real Miller-Good method. Since the absorptive part of the nuclear potential cannot be neglected, we had to make use of a perturbative approach for the imaginary part of the potential. Thus the turning point is determined by the real part of the potential and the phase integral is taken along a real trajectory. The imaginary part only supplied a damping factor to each of the partial waves. This approximation is good if the imaginary part is small. If the Miller-Good method is found suitable for a realistic problem, it may eliminate in some cases a lengthy direct numerical calculation, particularly if the accuracy demanded is not too high. In this context, we have also applied the complex Miller-Good method to study the same problem.

In the actual calculation, we have made a departure from the usual trend in connection with the choice of the coulomb part of the potential. In the study of heavy ion collision, the coulomb part of the potential is usually

taken in an approximate way. The potential chosen is given by either (a) that between a point charge and a sphere of uniform density or (b) that between two uniformly charged spheres of appropriate radii. The approximation appears to be a good one when the nuclei are heavy and have Fermi type of charge distributions. However, it is not obvious why this approximation should be valid for light nuclei like ^{12}C, ^{16}O etc. which have been used as projectiles for many experiments. These p-shell nuclei have a modified harmonic well type of charge distribution, which cannot be represented well by a uniform distribution. It is well-known that the elastic scattering of heavy ions depend more crucially on the real part of the potential around a critical distance $R \sim 1.5\ (A_1^{\frac{1}{3}} + A_2^{\frac{1}{3}})$ fm. Thus the elastic scattering normally places a very weak constraint on the detailed structure of the potential. However, considering also phenomena like the fusion and the nucleon transfer reactions one can determine the potential more accurately. The choice of the correct coulomb potential will, therefore, be more useful when the entire range of experimental results (elastic scattering, fusion and transfer reactions) are sought to be explained with the same set of potential parameters. It seems, therefore, worthwhile to see if the inaccuracy in the charge distribution chosen is reflected in the measurable quantities, particularly in the scattering cross-sections. With this view in mind we have considered here two cases: (A) the case of two uniformly charged spheres of radii $\sqrt{5/3}\ R_{r.m.s.}$ and (B) the case

of the two diffuse charge distributions of the modified harmonic well type. The coulomb potential in both the cases can be calculated analytically by making use of the convolution theorem of Fourier transforms. The nuclear potential between the nuclei was assumed to be given by a complex Woods-Saxon function. The phase shifts and the scattering cross-sections for a pair of p-shell nuclei (^{16}O - ^{16}O) were then calculated by the generalized semiclassical method. The results indicate some difference in phase shifts and in cross-sections in the cases (A) and (B). It may, therefore, be worthwhile to work with the correct charge distribution instead of the approximate distribution(A), which is commonly used in heavy ion codes[1].

The presentation of the material is as follows. In section IV.2., we have given the expressions for the coulomb potential between two colliding nuclei. The semiclassical method has been discussed in section IV.3. The calculated results are presented and analysed in section IV.4. In the next section, we shall study the ^{16}O - ^{16}O elastic scattering by the complex Miller-Good (CMG) method. The results will be compared with other results, theoretical and experimental. Our conclusions are also summarized there.

IV.2. The coulomb potential

To calculate the coulomb potential between the colliding nuclei we make use of the following results:

If the charge form factors of the nuclei A and B are $f_1(\vec{q})$ and $f_2(\vec{q})$, $\vec{q}$ being the momentum

transferred, the potential between them in momentum space is given by

$$V(\vec{q}) = \frac{4\pi}{q^2} Z_1 Z_2 e^2 \; f_1(\vec{q}) \; f_2(\vec{q}) \qquad \ldots(4.1)$$

The expression (4.1) follows easily from the convolution theorem of Fourier transforms. The potential in the coordinate space is given by

$$V_c(\vec{r}) = \frac{1}{(2\pi)^3} \int d^3q \; e^{-i\vec{q}\cdot\vec{r}} \; V(\vec{q}) \quad , \qquad \ldots(4.2)$$

and if the charge distribution is spherically symmetric,

$$V_c(r) = \frac{2 Z_1 Z_2 e^2}{\pi r} \int_0^\infty dq \left(\frac{\sin qr}{q} \right) f_1(q) \; f_2(q) . \qquad \ldots(4.3)$$

We shall consider two special cases:

Case I: When the colliding nuclei have charge distributions given by the generalized shell model (GSM).

It has been generally accepted[2] that for nuclei with an incomplete $1p$ shell, the charge distribution is given by

$$\rho(r) = \frac{2}{\pi^{3/2}} \; \frac{1}{a_0^3 (2 + 3\alpha)} \left(1 + \alpha \frac{r^2}{a_0^2} \right) \exp\left(-r^2/a_0^2 \right) , \qquad \ldots(4.4)$$

where

$$a_0 = \left(\frac{\hbar^2}{M\epsilon} \right)^{\frac{1}{2}} , \qquad \ldots(4.5)$$

ϵ being the energy interval between two consecutive levels of the harmonic oscillator. The root mean square radius (a) of the distribution is given by

$$a = a_0 \sqrt{\frac{3(2+5\alpha)}{2(2+3\alpha)}} \qquad \ldots(4.6)$$

with

$$\alpha = \frac{1}{3}(Z-2) \qquad \ldots(4.7)$$

The form factor for the distribution (4.4) can be easily evaluated and is seen to be given by

$$F(q) = \left[1 - \left(\frac{\alpha q^2 a_0^2}{2(2+3\alpha)} \right] \exp\left(- \frac{q^2 a_0^2}{4} \right) \right. \qquad \ldots(4.8)$$

Assuming that both the nuclei have charge distributions of the type (4.4), we have calculated the coulomb potential exactly by using the relation (4.3). This can be written as

$$V_c(r) = Z_1 Z_2 e^2 \left[\frac{1}{r} \mathrm{Erf}\left(\frac{r}{2B} \right) + (\beta + \gamma r^2) e^{-r^2/4B^2} \right] \qquad \ldots(4.9)$$

where

$$\beta = \left[3\, A_1 A_2 - 2(A_1 + A_2)\, B^2 \right] \;/\; 4B^5\sqrt{\pi} \qquad \ldots(4.10)$$

$$\gamma = -\, A_1 A_2 \;/\; 8B^7\sqrt{\pi} \qquad \ldots(4.11)$$

$$B^2 = B_1^2 + B_2^2 \qquad \ldots(4.12)$$

with

$$A_i = \alpha_i\, a_{oi}^2 \;/\left[2 + (2 + 3\alpha_i)\right] \qquad \ldots(4.13)$$

$$B_i^2 = a_{oi}^2/4 \quad , \qquad \ldots(4.14)$$

the suffix i (i = 1,2) refering to the i-th nuclei.

Case II: When the colliding nuclei have uniform charge distributions:

The charge distribution here is given by

$$\begin{aligned} \rho(r) &= \rho_o \quad \text{for} \quad r < R \\ &= 0 \quad \text{for} \quad r > R \end{aligned} \qquad \ldots(4.15)$$

R being the radius of the charged sphere. The corresponding form factor is given by

$$f(q) = \frac{1}{q^3 R^3}\left[\sin qR - qR\cos qR\right] \qquad \ldots(4.16)$$

From (4.3) and (4.16) one gets[3]

(i) for $r > R_1 + R_2$,

$$V_c(r) = \frac{Z_1 Z_2 e^2}{r} \qquad \ldots(4.17)$$

(ii) for $r < R_1 - R_2$,

$$V_c(r) = \frac{Z_1 Z_2 e^2}{R_1} \left[\frac{3}{2} - \frac{1}{2} \frac{r^2}{R_1^2} - \frac{3}{10} \frac{R_2^2}{R_1^2} \right] \qquad \ldots(4.18)$$

(iii) for $R_1 - R_2 < r < R_1 + R_2$,

$$V_c(r) = Z_1 Z_2 e^2 \left[\frac{1}{r} + \frac{1}{160\, r\, (p_1 p_2)^3} \sum_{j=0}^{6} C_j (p_1 + p_2)^j \right] \qquad \ldots(4.19)$$

where

$$p_i = \frac{R_i}{r}, \quad i = 1,2 \qquad \ldots(4.20)$$

and

$$C_0 = -30\,P_1P_2 - 1$$

$$C_1 = 120\,p_1p_2$$

$$C_2 = 15 - 180\,p_1p_2$$

$$C_3 = 120\,p_1p_2 - 40$$

$$C_4 = 45 - 30\,p_1p_2$$

$$C_5 = -24$$

$$C_6 = 5\,. \qquad \ldots(4.21)$$

For two identical nuclei, the potential can be written in a simpler form, viz:

$$V_c(r) = \frac{Z^2e^2}{r}\left\{1 + \frac{1}{160\,R^6}\,(30\,r^4R^2 - r^6 - 80\,R^3r^3 + 192\,R^5r - 160\,R^6)\right\}, \qquad r < 2R$$

$$= \frac{Z^2e^2}{r}\,, \qquad r > 2R \qquad \ldots(4.22)$$

We shall do the calculations here with both the potentials (Case I) and (Case II). The nuclear part of the potential for $^{16}O - ^{16}O$ will be taken to be a complex optical model potential, as chosen by Maher et al[4], viz;

$$V_N(r) = \frac{-(V_o + i\,W_o)}{1 + \mathrm{Exp}\left(\frac{r - R_o}{a_o}\right)} \qquad \ldots(4.23)$$

with W_o depending on the collision energy.

IV.3. Semiclassical phase shifts and cross-sections

We shall consider here a perturbative method for treating the complex optical potential, assuming that the imaginary part of the potential is small. Thus instead of working with the wave vector

$$K(r) = \left[K^2 - \frac{2\mu}{\hbar^2} (V_R + i\,V_I) - \frac{L(L+1)}{r^2} \right]^{\frac{1}{2}}, \qquad \ldots(4.24)$$

we expand and keep terms upto first order in V_I. The contribution of the imaginary part in this approximation is contained in a damping factor $e^{-2S(L)}$ for each partial wave of angular momentum L, where

$$S(L) = \frac{2\mu}{\hbar^2} \int_{r_o}^{\infty} \frac{V_I\, dr}{2\left[K^2 - \frac{2\mu}{\hbar^2} V_R - \frac{L(L+1)}{r^2}\right]^{\frac{1}{2}}} \qquad \ldots(4.25)$$

Apart from this damping factor, the problem is now that of a real potential. Consequently, the turning point and

the trajectory are both real and the generalized semiclassical method can be applied to this problem in a straightforward manner. The parameters chosen for the Woods-Saxon potential[4] for ^{16}O - ^{16}O scattering indicate that W_o is indeed much smaller than V_o, at least upto about E_{cm} = 50 Mev. Thus, the approximation made above may be acceptable.

The details of the semiclassical method have already been given in chapter II. The method has been found to give accurate results even at low energies, where the conventional JWKB method is inaccurate. We shall consider only terms of lowest order in $\hbar^2$. We have chosen as the model equation, the radial equation for scattering from a point charge with the same Sommerfeld parameter,

$$n = \frac{2\mu}{\hbar^2} \frac{Z_1 Z_2 e^2}{2K} , \qquad \ldots(4.26)$$

where $K^2\hbar^2/2\mu$ is the C.M. energy. To obtain an expression for the phase shifts, we first write the radial equation for the problem as

$$\frac{d^2R_L(y)}{dy^2} + \frac{t_1(y)}{\hbar^2} R_L(y) = 0 , \qquad \ldots(4.27)$$

with

$$\frac{1}{\hbar^2} t_1(y) = 1 - \frac{L(L+1)}{y^2} - \frac{2\mu}{\hbar^2 K^2} (V_N + V_c) , \qquad \ldots(4.28)$$

where $y = Kr$ and $V_N(y)$ and $V_c(y)$ are the nuclear and coulomb part of the potential respectively. The model equation is also written as

$$\frac{d^2 R^o_L(s)}{ds^2} + \frac{t_2(s)}{\hbar^2} R^o_L(s) = 0, \qquad \ldots(4.29)$$

with

$$\frac{1}{\hbar^2} t_2(s) = 1 - \frac{2n}{s} - \frac{L(L+1)}{s^2} . \qquad \ldots(4.30)$$

Let us now introduce Langer's substitution

$$y = e^x ,$$

$$R_L(y) = e^{x/2} G_L(x) \qquad \ldots(4.31)$$

to obtain the transformed radial equation for the problem as

$$\frac{d^2 G_L(x)}{dx^2} + \frac{q_1(x)}{\hbar^2} G_L(x) = 0, \qquad \ldots(4.32)$$

where

$$\frac{1}{\hbar^2} q_1(x) = e^{2x} \left[1 - \frac{2\mu}{\hbar^2 K^2} V'_c(x) - \frac{2\mu}{\hbar^2 K^2} V'_N(x) \right] - \left(L + \frac{1}{2} \right)^2 \qquad \ldots(4.33)$$

where $V_N'(x)$ and $V_c'(x)$ are the potentials in the new variable. We can make a similar transformation for the model equation, Viz;

$$s = e^Z ,$$

$$R_L^o(s) = e^{Z/2} G_L^o(Z) \qquad \ldots(4.34)$$

to obtain the transformed model equation as

$$\frac{d^2 G_L^o(Z)}{dZ^2} + \frac{q_2(Z)}{\hbar^2} G_L^o(Z) = 0 \qquad \ldots(4.35)$$

where

$$\frac{1}{\hbar^2} q_2(Z) = e^{2Z} - 2ne^Z - (L + \tfrac{1}{2})^2 . \qquad \ldots(4.36)$$

We now apply the Miller-Good method to the set of equations (4.32) and (4.35). The phase shifts in the zeroth order can be expressed in terms of the original variables as

$$\sigma_L^o = \sigma_L^c + \sigma_L^{diff} \qquad \ldots(4.37)$$

where

$$\sigma_L^c = \mathrm{Arg}\,\Gamma(L + 1 + in) , \qquad \ldots(4.38)$$

and

$$\sigma_L^{diss} = (L + \tfrac{1}{2}) \left[\frac{\pi}{2} - \sin^{-1} \left(\frac{n\breve{y} + (L + \frac{1}{2})^2}{\breve{y}\sqrt{n^2 + (L + \frac{1}{2})^2}} \right) \right]$$

$$+ n \ln \left(\frac{\breve{y} - n + \sqrt{\breve{y}^2 - 2n\breve{y} - (L + \frac{1}{2})^2}}{\sqrt{n^2 + (L + \frac{1}{2})^2}} \right)$$

$$- \sqrt{\breve{y}^2 - 2n\breve{y} - (L + \tfrac{1}{2})^2} + \int_{y_t}^{\breve{y}} \sqrt{t_1(y)}\, dy \qquad \ldots(4.39)$$

where y_t is the classical turning point, and $\breve{y}$ is a large value of y, which we choose. The choice is such that the total potential between the two nuclei is given very accurately by only the coulomb term $2n/\breve{y}$.

One of the problems in working with a semi-classical method is to decide on the turning points that has to be taken into account in calculating the phase shifts. Here, we follow the prescriptions of Knoll and Schaeffer, who made a systematic analysis of this problem. For intermediate energies, there is a range of L values for which there are three real roots of $\eta_1(x) = 0$. We have shown in Fig. 4.1 the effective potential with the charge distribution (4.9). We have also shown in Fig. 4.2 and Fig. 4.3 a typical case for the C.M. energy E_{cm} = 31.5 Mev and for a potential given by (4.9) and (4.22). According to the criterion of Knoll and Schaeffer, for L values lower than the orbiting value

Fig. 4.1. The effective potential $V_{eff}(r)$ which includes the real part of the nuclear potential, the centrifugal term and the coulomb field generated by GSM charge distribution, for different values of L.

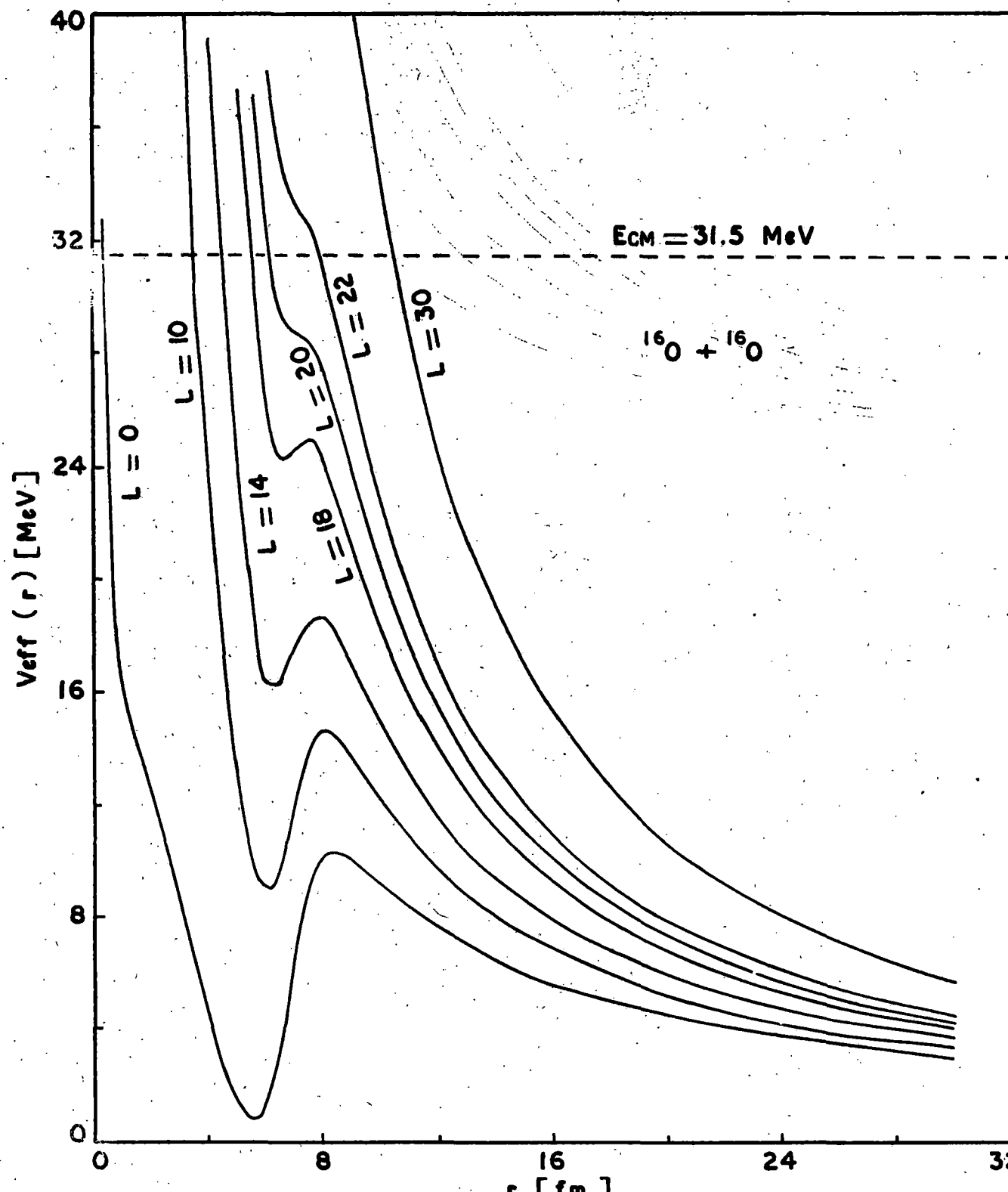
40
32
24
16
8
0
Veff (r) [MeV]
Ecm = 31.5 MeV
16O + 16O
L = 0
L = 10
L = 14
L = 18
L = 20
L = 22
L = 30
0
8
16
24
r [fm]

FIG. 4.1.

Fig. 4.2. The real function $t_1(y)$ for different values of L with GSM coulomb charge distribution at E_{cm} = 31.5 Mev.

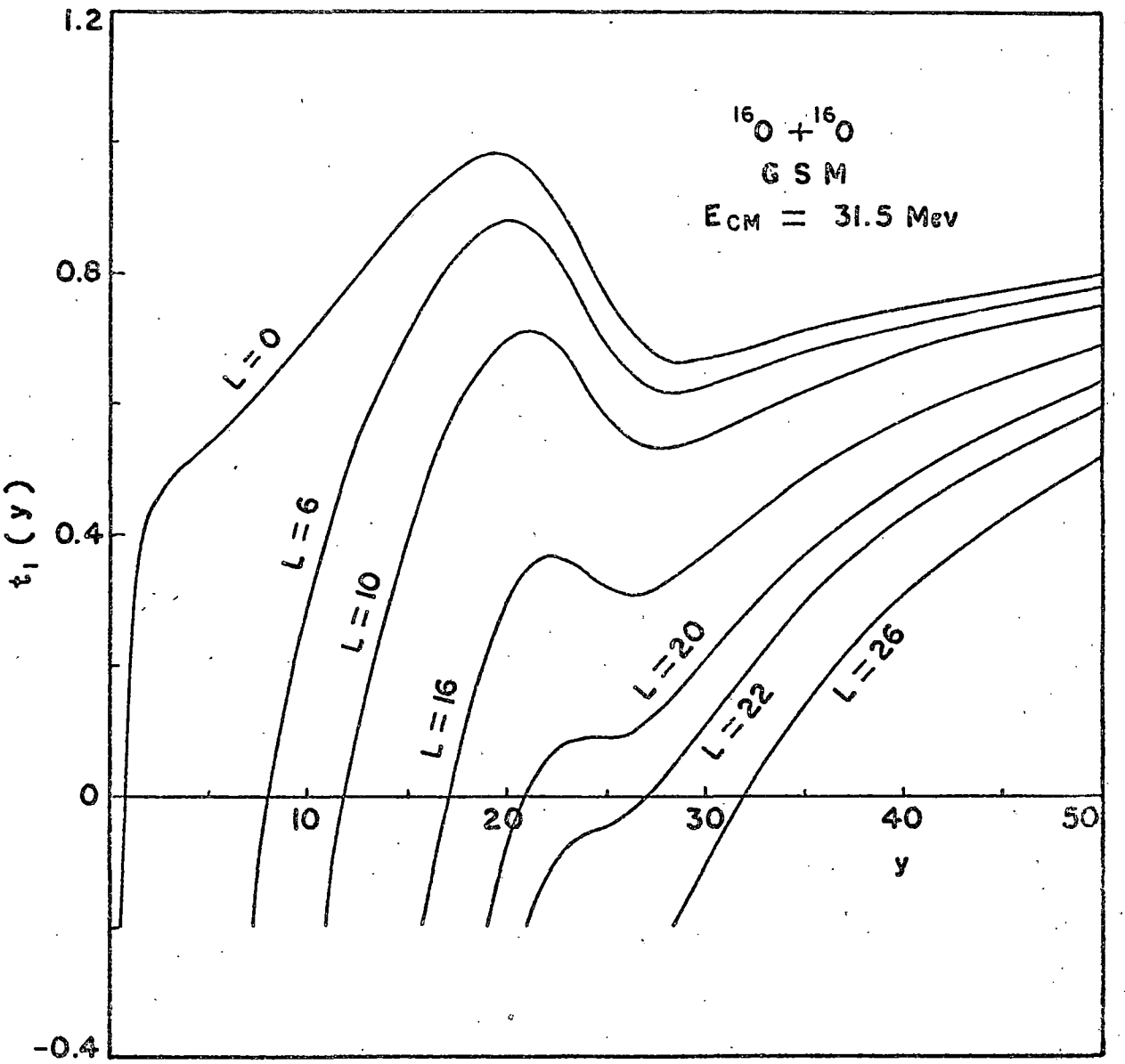
1.2
0.8
0.4
0
-0.4
$t_1(y)$
$^{16}O + ^{16}O$
G S M
$E_{CM} = 31.5$ Mev
L=0
L=6
L=10
L=16
L=20
L=22
L=26
10
20
30
40
50
y

FIG. 4.2 .

Fig. 4.3. The real function $t_1(y)$ for different values of L with uniform coulomb charge distribution at E_{cm} = 31.5 Mev.

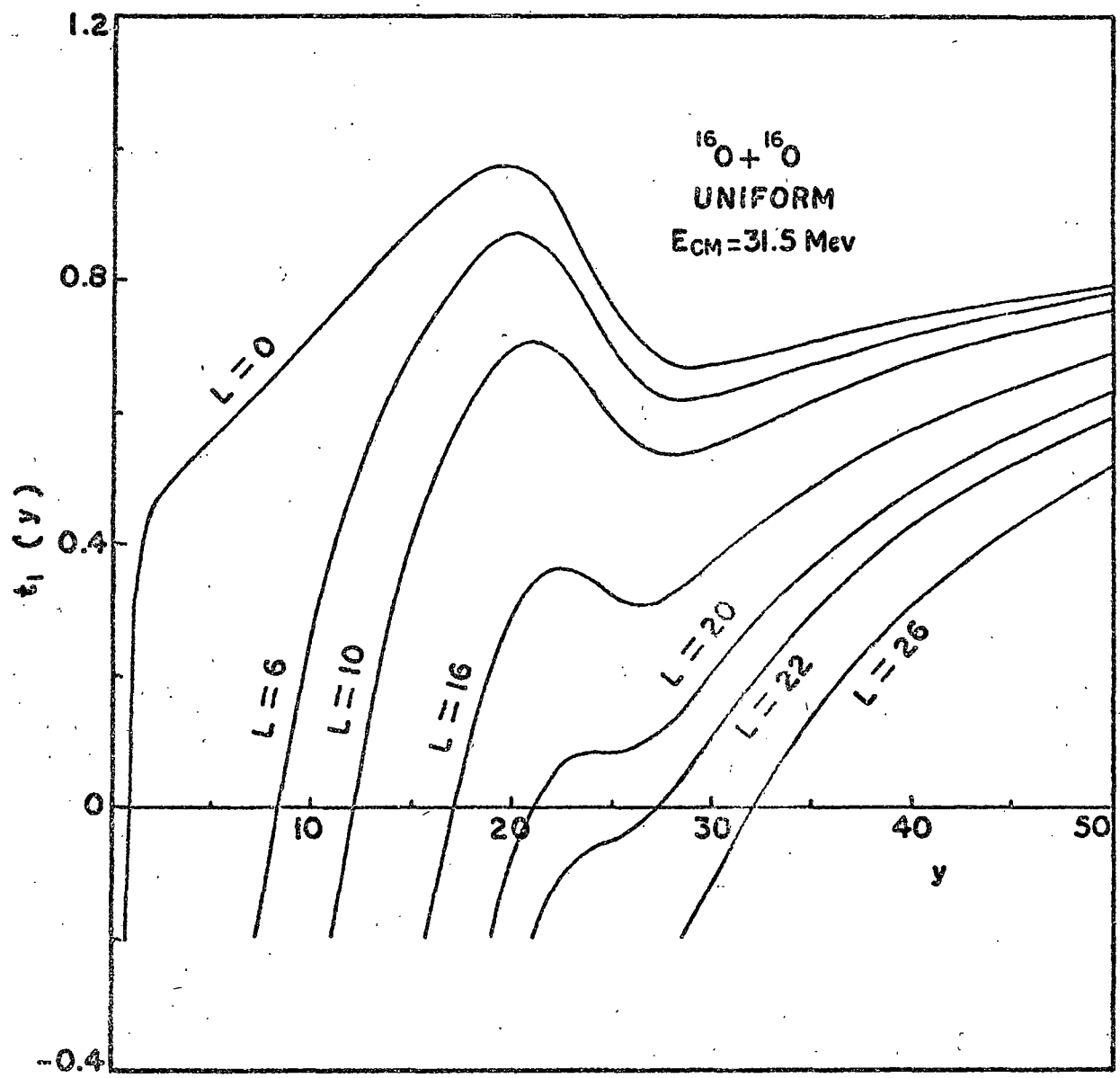
1.2
0.8
0.4
0
-0.4
$t_l(y)$
$^{16}O + ^{16}O$
UNIFORM
E_{CM} = 31.5 Mev
L=0
L=6
L=10
L=16
L=20
L=22
L=26
10
20
30
40
50
y

FIG. 4.3.

(when the maximum of the potential barrier equals E_{cm}), it is the inner turning point r_2 which contributes. At the orbiting value L_{orbit}, the phase shift jumps, since then the outer turning point r_1 alone starts giving the phase shift. At higher energies there is one real turning point which contributes. It may be pointed out that even for a real potential, one has complex turning points, which should, in principle, contribute for L values for which a pocket in the potential appears. Physically, this contribution accounts for the quantum mechanical reflection of the wave passing over a potential barrier. However, the effect of this term is small and we will not consider it in the calculation that follows. The problem of the choice of turning points for the complex trajectories is more involved and will be taken up in section.IV.5.

To calculate the cross-sections, one has to take into account the symmetry of the projectile and the target. Thus, one can write for the amplitudes,

$$\tilde{f}(\theta) = f(\theta) + f(\pi - \theta)$$
$$= \tilde{f}_M(\theta) + \frac{1}{iK}\sum_{L\,\text{even}} (2L+1)\left(e^{-2S(L)}e^{2i\delta_L} - e^{2i\delta_L^c}\right) P_L(\cos\theta$$

...(4.40)

where S(L) is given by (4.25) and $\tilde{f}_M(\theta)$, the

symmetrized Mott scattering amplitude is given by

$$\tilde{f}_M(\theta) = -\frac{n}{2K}\left[\frac{\cos\alpha}{\sin^2\theta/2} + \frac{\cos\beta}{\cos^2\theta/2}\right]$$

$$-i\frac{n}{2K}\left[\frac{\sin\alpha}{\sin^2\theta/2} + \frac{\sin\beta}{\cos^2\theta/2}\right] \qquad \ldots(4.41)$$

with

$$\alpha = 2\delta_o^c - n\ln\sin^2\frac{\theta}{2}\,, \qquad \ldots(4.42)$$

$$\beta = 2\delta_o^c - n\ln\cos^2\frac{\theta}{2}\,, \qquad \ldots(4.43)$$

and

$$\delta_o^c = \operatorname{Arg}\Gamma(1+in)\,. \qquad \ldots(4.44)$$

The ratio σ_{el}/σ_M of the symmetrized scattering cross-sections can be easily calculated from the above relations. The summation in (4.40) can be terminated for a value of L so that all higher δ_L and δ_L^c differ by a quantity which is less than a preassigned small number.

IV.4. Results and discussions

We have calculated the phase shifts as well as the scattering cross-sections for the $^{16}O - ^{16}O$ elastic scattering in the energy range $E_{cm} = 26.5 - 43.5$ Mev. The potential parameters were chosen as follows:

1. For the GSM charge distribution:

   $\alpha = 2$, $a = 2.625$ fm.

2. For the uniform charge distribution:

   $R = 3.39$ fm.

3. The parameters for the nuclear potential were as follows[4]:

   $V_o = 17$ Mev, $W_o = 0.4 + 0.1\ E_{cm}$

   $R_o = 6.8$ fm, $a_o = 0.49$ fm.

The phase shifts were calculated explicitly upto L = 100, beyond which the phase shifts were assumed to be given by the coulomb phase shifts. Some of the real turning points for certain values of angular momenta are shown in Table VII. These turning points were used in evaluating the integral of equation (4.39). Our results are as follows:

(a) Phase shifts and its variation with energy:

The calculated phase shifts show a smooth variation with energy. Some phase shifts with G S M charge

TABLE VII. Turning points (real) with G S M and uniform Coulomb charge distributions. The nuclear potential is real and as given in ref. 4.

L	Real turning points y_t	
	G S M	UNIFORM
0	0.724	0.704
2	3.499	3.416
4	5.955	5.856
6	8.118	8.038
8	10.075	10.026
10	11.895	11.876
12	13.628	13.633
14	15.314	15.333
16	16.996	17.020
18	18.751	18.776
20	20.876	20.897
22	27.190	27.191
24	29.866	29.866

distribution at different energies are shown in Fig. 4.4.

(b) Effect of the imaginary potential:

The effect of the imaginary potential is to supply a damping factor to each of the partial waves. In the present problem, (E_{cm} = 31.5 Mev) partial waves upto L $\backsim$ 24 are affected, the higher partial waves are not absorbed. The effect of this damping on the scattering cross-sections is shown in Tables VIII and IX.

(c) Effect of charge distribution:

The phase shifts for the G S M charge distribution and the uniform charge distribution show slight differences as shown in Table X, particularly for low values of L. For higher values of L(L $\backsim$ 26 and upwards) the difference almost vanishes, as expected. The results indicate that one will have to alter the radius of the uniform distribution appreciably, if one wants to fit the G S M results with a uniform model. This may be possible, since the scattering does not depend critically on the potential excepting in a certain region, mostly on the tail of the potential. But the consequent change of potential elsewhere may be reflected in the cross-sections for other processes, viz. fusion or transfer processes. It is, therefore, useful to consider the realistic G S M charge distribution in the study of heavy ion collision processes with nuclei like ^{16}O and ^{12}C.

Fig. 4.4. Variation of the semiclassical phase shifts with energy for elastic $^{16}O - ^{16}O$ scattering. The potential chosen is given by Maher et al.[4]

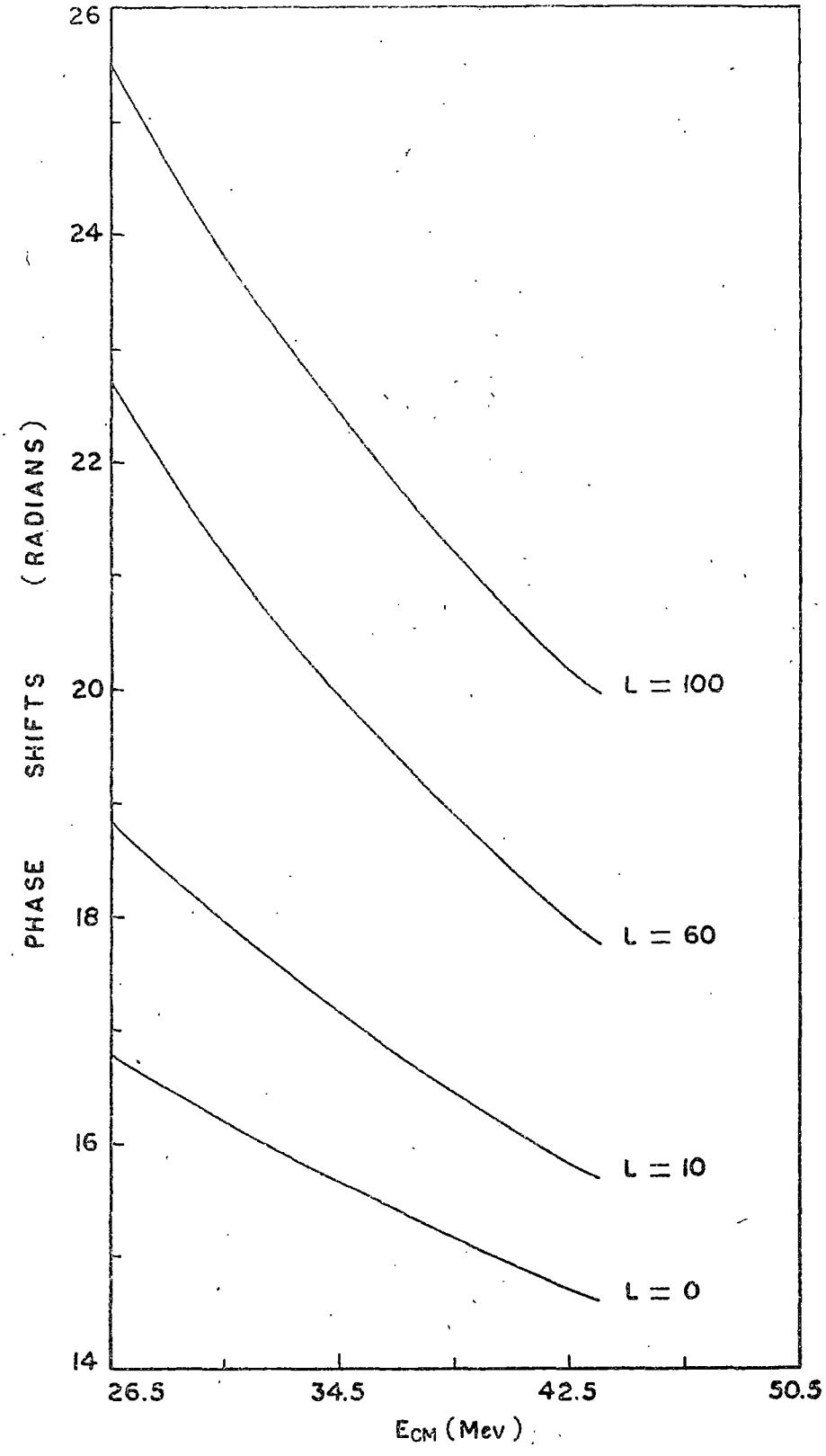
26
24
22
20
18
16
14
PHASE SHIFTS (RADIANS)
L = 100
L = 60
L = 10
L = 0
26.5
34.5
42.5
50.5
ECM (Mev)

FIG. 4.4.

TABLE VIII. ^{16}O - ^{16}O elastic scattering cross-sections with G S M coulomb charge distribution.

θ_{cm} (degrees)	$d\sigma_{el}/d\sigma_{MOTT}$ (with $W_o = 0.0$)	$d\sigma_{el}/d\sigma_{MOTT}$ (With $W_o = 0.4 + 0.1\ E_{cm}$)
20	0.241	0.241
25	0.193	0.196
30	0.999	0.992
35	0.023	0.022
40	0.912	0.925
45	0.426	0.424
50	0.328	0.320
55	0.494	0.499
60	0.087	0.091
65	0.901	0.890
70	0.643	0.648
75	2.588	2.632
80	0.793	0.784
85	0.049	0.047
90	0.464	0.469

TABLE IX. ^{16}O - ^{16}O elastic scattering cross-sections with Uniform coulomb charge distribution.

θ_{cm} (degrees)	$d\sigma_{el}/d\sigma_{MOTT}$ (With $W_o = 0.0$)	$d\sigma_{el}/d\sigma_{MOTT}$ (With $W_o = 0.4 + 0.1\ E_{cm}$)
20	0.223	0.224
24	0.466	0.471
28	0.310	0.307
32	0.839	0.834
36	0.036	0.037
40	0.873	0.883
44	0.204	0.208
48	0.848	0.841
52	0.063	0.060

TABLE X. The phase shifts for ^{16}O - ^{16}O elastic scattering with G S M and Uniform Coulomb charge distributions. The nuclear potential is given by a Woods-Saxon potential[4].

L	Phase shifts (radians)	
	G S M	UNIFORM
0	16.051	16.195
2	16.244	16.366
4	16.605	16.687
6	17.018	17.060
8	17.409	17.421
10	17.736	17.728
12	17.968	17.950
14	18.078	18.057
16	18.029	18.011
18	17.760	17.746
20	17.114	17.106
22	16.110	16.200
24	16.358	16.358

IV.5. Complex Miller-Good Method

In this section, we shall consider the complex Miller-Good (CMG) method for studying the ^{16}O - ^{16}O elastic scattering phenomena. For simplicity, we shall consider energies for which there is only one contributing complex trajectory. This makes it necessary to consider an energy greater than 25 Mev in the C.M. frame. We have chosen the optical potential parameters given by Maher et al. It is known that this potential does not reproduce the experimental results, at the energies considered but our aim here is limited to the study of the efficacy of the CMG method in the case of a realistic scattering phenomenon. We have considered the scattering at E_{cm} = 31.5 Mev in detail and compared our results with (i) the results obtained by the perturbative method, discussed in the last section, (ii) the exact results and (iii) the experimental results. The last two results have been taken from Maher et al.

In applying the CMG method, the first step is to select the complex turning points which will make the dominant contribution. In the case considered, the complex turning point turns out to be the analytic continuation in the complex plane of the zeros of the function Re $t_1(y) = 0$, which are first calculated. We have shown in Fig. 4.5 the complex roots considered for calculating

Fig. 4.5. Some complex turning points for different values of L for the ^{16}O - ^{16}O system at E_{cm} = 31.5 Mev with GSM coulomb charge distribution. The nuclear parameters are as in Ref. 4.

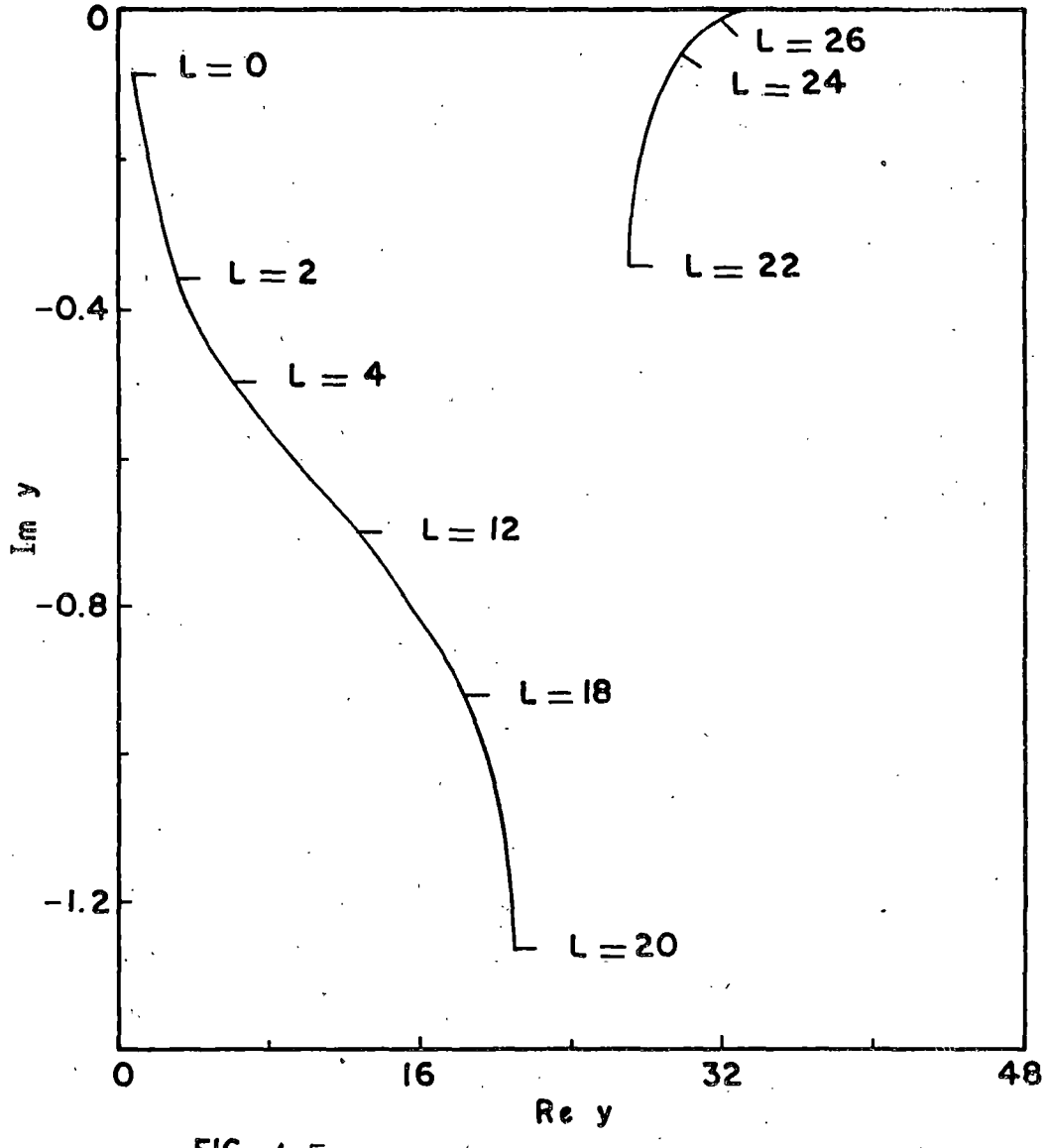

FIG. 4.5.

the phase shifts. These have been determined by an iterative method, giving the real root of Re $t_1(y)$ as an input. Our choice of the roots are consistent with the prescription of Knoll and Schaeffer. The path-integrations have been done along the contour shown in Fig. 2.1. The differential cross-section is calculated by considering (i) complex phase shifts upto L = 20, (ii) perturbative semiclassical phase shifts for L = 22 to L = 100, and (iii) coulomb phase shifts for larger L. The radial waves for L = 22 and higher are not much absorbed so that it is sufficient to consider complex integration upto L = 20.

We have shown the differential cross-section in Fig. 4.6 at E_{cm} = 31.5 Mev. The solid line gives the CMG results obtained as in above, while the dashed curve gives the results obtained by the perturbative method. The dotted line gives the experimental results of the Yale group.[4-6] The CMG results seem to give better agreement with the experimental results than the perturbative method, though the agreement is still poor. This is not surprising, because even the exact numerical calculation of Maher et al. shows poor agreement with the data (Fig. 4.7). The weakness of the potential is evident from the structure of the theoretical cross-section near 50° and 80°, which are out of phase with the experimental results. The approximate results obtained by us show almost the same features. However, the number and positions of the peaks

TABLE XI. Some complex turning points with GSM coulomb charge distribution for ^{16}O - ^{16}O system at E_{cm} = 31.5 Mev. The nuclear potential is as given by Maher et al.

L	Real part	Imaginary part
0	0.7092	-0.0823
2	3.4478	-0.3548
4	5.9005	-0.5043
6	8.0682	-0.5808
8	10.0285	-0.6288
10	11.8501	-0.6683
12	13.5830	-0.7082
14	15.2664	-0.7544
16	16.9411	-0.8169
18	18.6761	-0.9276
20	20.6635	-1.2689
22	27.2648	-0.3408
24	29.8674	-0.0568
26	31.9916	-0.0160
28	34.0080	-5.0380 E-03
30	35.9950	-1.6309 E-03
32	37.9747	-5.3160 E-04
34	39.9537	-1.7329 E-04
36	41.9341	-5.6378 E-05
38	43.9161	-1.8299 E-05
40	45.8998	-5.9257 E-06

Fig. 4.6. Differential cross-section for ^{16}O - ^{16}O elastic scattering. The solid line represents the cross-section obtained by the CMG method and the dashed line by the perturbative treatment. The dotted line joins the data points of Ref. 4.

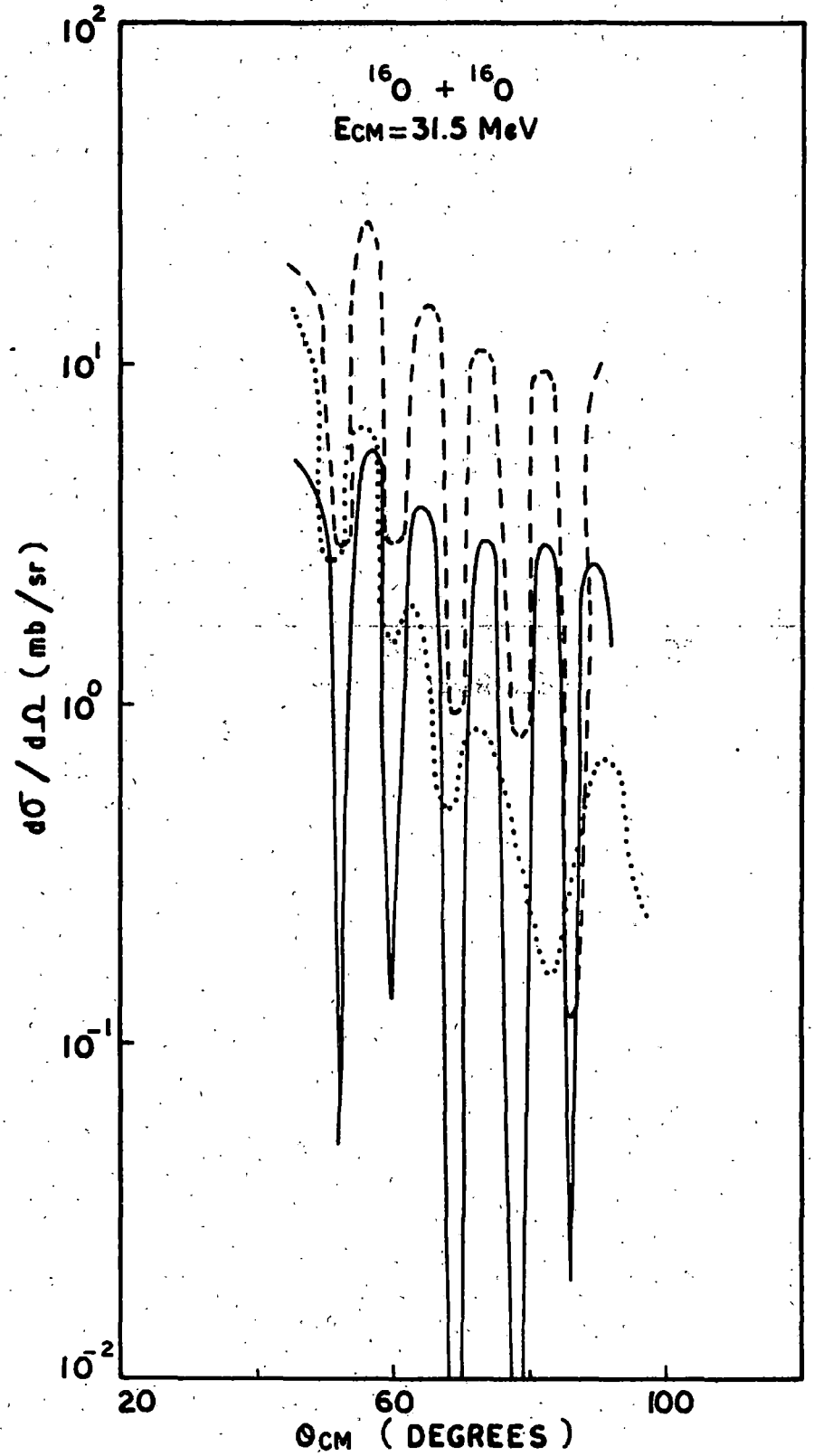
$^{16}O + ^{16}O$
$E_{CM} = 31.5$ MeV
10^2
10^1
10^0
10^{-1}
10^{-2}
$d\sigma / d\Omega$ (mb/sr)
20
60
100
θ_{CM} (DEGREES)

FIG. 4.6.

Fig. 4.7. $^{16}O - {}^{16}O$ elastic scattering angular distributions reproduced from Ref. 4. The solid line gives the exact results and the dashed curve interpolates the experimental points.

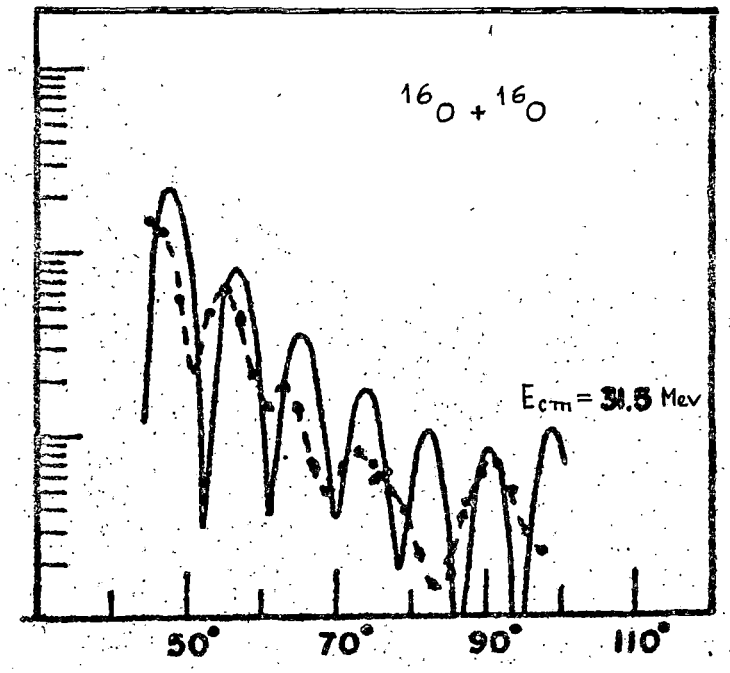

FIG. 4.7.

obtained by the approximate methods seem to agree well with the exact results, though there are still quantitative discrepancies, particularly near the minima, where correction terms of order $\hbar^2$ should have been considered.

It has been suggested that the shallow 17 Mev optical potential is not adequate and either a repulsive core and/or an ℓ-dependant potential is needed along with this shallow potential. Halbert et al[7], following this suggestion, was able to get a better fit with the experimental results at higher energies. It is however, beyond the scope of the present work to aim for an accurate fitting of the potential. We would rather summarise our conclusions in the following:

The Complex Miller-Good method is an accurate method for determining the phase shifts, where the method is applicable in a simple way. However, the cases where the real part of $t_1(y)$ has three or more real zeros, the computation of the phase shifts becomes involved. Since in the semiclassical method, each radial equation has its own special feature and has to be studied separately, it is obviously not a good alternative to an exact numerical calculation. The semiclassical calculation, nevertheless, may serve a useful purpose, by giving an approximate estimate of the phase shifts and cross-sections[8]. The general feature revealed by these approximate calculations may be used as a guide for a subsequent numerical

computation. Moreover, where the gross features of the scattering are all that are needed to be known, the semiclassical method has already proved its utility. For scattering from simple potentials, the semiclassical methods often provide various bounds or exact results. Already in the realm of particle physics, the semiclassical approximations have found useful applications, particularly in the description of heavy quarkonia, the bound states of a quark and its antiquark. These states can be described in terms of a Schrödinger's equation, because at small distances the interaction potential which confines the quarks is small compared to the constituent quark masses. A number of useful bounds and exact results have been obtained here from semiclassical considerations.[9] The heavy ion scattering processes are, of course, more complex in nature. Still, it is expected that the semiclassical methods, because of its basic simplicity, can be quite useful in studying at least the gross features of these complex manybody processes.

REFERENCES

1. M. H. Macfarlane and S. C. Pieper, ANL. Reports No. 76-96 (1976).

2. R. Hofstadter, Revs. Mod. Phys. 28, 214 (1956).

3. G. C. Oades and G. Rasche, unpublished Rutherford Preprint RPP/T/1 (1977).

4. J. V. Maher, M.W. Sachs, R. H. Siemssen, A. Weidinger and D.A. Bromley, Phys. Rev. 188, 1665 (1969).

5. R. H. Siemssen, J.V. Maher, A. Weidinger and D.A. Bromley, Phys. Rev.Letts. 19, 369 (1967).

6. W. Reilly, R. Wieland, A. Gobbi, M.W.Sachs and D.A. Bromley, IL Nuovo Cimento, 13, 897 (1973).

7. M. L. Halbert, C.B. Fulmer, S. Raman, M.J. Saltmarsh, A.H. Snell and P.H. Stelson, Phys. Letts. 51B, 341 (1974)

8. P. C. Sood, C. Maheswari, S. Mukherjee and R.K.Samanta, Proc. Int. Conf. on Nucleus - Nucleus collisions (Michigan) Vol.1, pp.79 (1982).

9. H. Grosse and A. Martin, Phys. Rep. 60, 343 (1980), and the references given therein.